Adaptive beamforming algorithms for a 60 GHz multiple antenna receiver

van der Kuijp, H.P.

Award date:
2006

Eindhoven University of Technology
Department of Electrical Engineering
Signal Processing Systems

TU/e technische universiteit eindhoven

Adaptive beamforming algorithms for a 60 GHz multiple antenna receiver

by H.P. van der Kuijp

Master of Science thesis

Project period: July 2005 – February 2006
Report Number: 05 - 06

Commissioned by:

Prof. Dr. Ir. J.W.M. Bergmans (TU/e)

Supervisors:
Dr. Ir. F.M.J. Willems (TU/e)
Dr. R. Rietman (Philips)

Abstract

The 60 GHz frequency band link budget limitations impose the use of high gain antennas for high data rate communication. High gain antennas, mostly antenna arrays, imply beamforming and in order to create beams in the required direction, the antennas need to be steerable.

In this master thesis report adaptive beamforming algorithms, based on a generic 60 GHz multiple antenna receiver architecture, have been developed.

The receiver architecture is characterized by a combined digital baseband output and beam steering at RF.

The developed beamforming algorithms may be divided into maximization of signal-to-noise ratio (SNR) beamforming and power controlled beamforming.

Maximization of SNR beamforming requires the channel statistics to be known. Channel estimation is used to perform signal combining at RF. The first algorithm, the rounding method, sets the phase shift in the RF path such that the resulting phase shift of the received signal is as small as possible. However, this result is not optimal, due to phase shift limitations. The optimized rounding method uses the solution of the rounding method to achieve an optimal solution.

Power controlled beamforming does not require channel statistics to be known. The antenna beam is set in a number of directions during which a training symbol is received. Based on the maximum received power the beam is set in the corresponding direction. Linear search beamforming sets the beam direction after performing one iteration, covering 360 degrees. Binary search beamforming sets the beam direction after a number of iterations, the first iteration covers 360 degrees, the following iterations uses the result of the preceding iterations, each iteration using more antennas, hence narrowing the beam.

Simulation of these beamforming algorithms, using 1 transmitter and a line of sight link, show that algorithms based on maximization of SNR beamforming achieve a slightly better result than power controlled beamforming. If no line of sight is present, the received signal phase of the antenna branches are not correlated due to the direction of arrival, maximization of SNR beamforming performance is hardly influenced whereas power controlled beamforming algorithms are no longer capable of beamforming.

Contents

Chapter 1

Introduction

The growing demand for high-speed wireless communications, in particular with large channel capacity for Quality of Service (QOS) multimedia applications, has led to the research on 60 GHz wireless data communication systems.

The 60 GHz band offers ample bandwidth, up to 7 GHz, and is the prime candidate for succeeding Ultra-Wideband (UWB) in the 3 to 10 GHz band as the demand for higher data rates continues. This spectrum is unlicensed, which means that for operating equipment one does not need to acquire a license from any governmental organization. The spectrum is a major improvement over the less than 0.3 GHz, currently available license free spectrum.

The 60 GHz frequency band benefits from a severe oxygen attenuation absorbtion, approximately 10-15 dB/km. This allows a higher frequency reuse and provides a more secure link, given the limited range. For indoor use, the near inability to transmit through walls provides the same benefits as the oxygen absorbtion.

A drawback for the performance of a 60 GHz communication system is the limited link budget. The received signal power, among others, depends on the antenna surface area. A carrier frequency of 60 GHz implies one wavelength to be 5 mm, hence the antenna surface area is very small compared to communication systems operating at a lower frequency. In order to boost the received signal power, the receiver may be designed with a multiple antenna system. To exploit the antenna array in full extent, the receiver must use a combining algorithm, also known as beamforming algorithm. This master's thesis report discusses and evaluates several forms of beamforming algorithms for a 60 GHz indoor wireless local area network (WLAN) system. [Koh, no year][Smulders, 2002]

1.1 Problem definition

In the 60 GHz frequency band link budget limitations impose the use of high gain antennas for high datarate communication over a distance of several meters. High gain antennas, mostly antenna arrays, imply beamforming and in order to create beams in the required direction, the antennas need to be steerable. Steering the antenna beam can be done by introducing switchable delays in each of the antenna branches.

The above scenario poses several research challenges, e.g.:

- design of preambles or sounding packets;
- design and analysis/simulation of antenna steering algorithms;
- signal processing, such as maximal ratio combining, at RF level;
- design and analysis of MAC protocols for a beamformed system.

This report will focus on item 2 and 3 and where applicable will mention item 1 and 4.

1.2 Research objective

Communication systems operating in the 60 GHz frequency band are still under research. In order to discuss and evaluate different beamforming algorithms, one common receiver design will be used.

The goal of beamforming is to maximize the signal-to-noise ratio (SNR) at the output of the receiver by appropriately choosing the gain and phase per receive path.

Based upon the receiver architecture, two types of adaptive beamforming algorithms will be developed:

- Beamforming using channel estimation
- Beamforming without channel estimation

Channel estimation can be separated in full channel estimation and partial channel estimation.

If any form of channel estimation is performed, combining techniques such as maximal-ratio combining (MRC) or equal-gain combining (EGC) may be used in the beamforming algorithm. [Haykin and Moher, 2005]

Without channel estimation, the beamforming algorithm needs to perform a scan in order to find out from which direction the optimum SNR at the output of the receiver can be achieved.

The objectives of this master thesis are as follows:

- Development of a full channel estimation technique
- Development of a partial channel estimation technique
- Development of a combining algorithm using channel estimation
- Development of a combining algorithm without channel estimation
- Simulation of the algorithms and comparison of their performance

1.3 Report outline

Before any algorithm can be developed, it is important to know the receiver design, this design is given in Chapter 2. In Chapter 3 some basic terminology is given and a number of common known beamforming and combining techniques are described. These techniques lead to maximization of signal-to-noise ratio beamforming and reference signal beamforming algorithms, which are studied in Chapter 4 and 5, respectively. These algorithms are simulated and the results are given in Chapter 6. Finally conclusions are drawn and recommendations are given in Chapter 7.

Chapter 2

Receiver architecture

In this chapter a generic architecture for a 60 GHz, multiple antenna receiver, will be described. At this moment receiver architecture is still a research topic. Combining algorithms, as developed in this thesis, should operate independently of the final receiver design provided a common interface between the receiver and combining logic is developed.

The receiver architecture can be divided in the following building blocks:

1. Antenna array
2. RF front-end
3. Analog-to-Digital conversion
4. Receiver logic

Figure 2.1 shows the generic receiver architecture as described in this chapter.

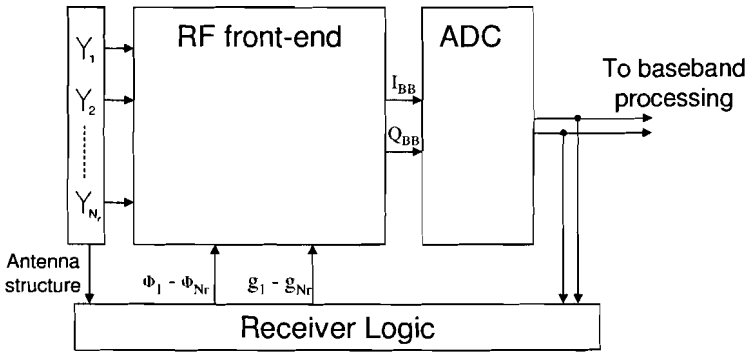

Figure 2.1: Generic receiver architecture

2.1 Antenna array

Antenna arrays can form beams and zeros in desired directions by controlling the time delay and gain of the signal in each path independently. In order to achieve the desired beamforming, the, relative, antenna placing must be known when developing the beamforming algorithms.

A feasible antenna array for the multiple antenna receiver is a linear antenna array or antenna planar. An antenna planar is in fact a combination of linear antenna arrays. Other antenna arrays, eg. circular, are possible. For the combining algorithm in this report it is chosen to use a linear antenna array consisting of N_r equally spaced isotropic antennas at distance d. [Haykin and Moher, 2005]

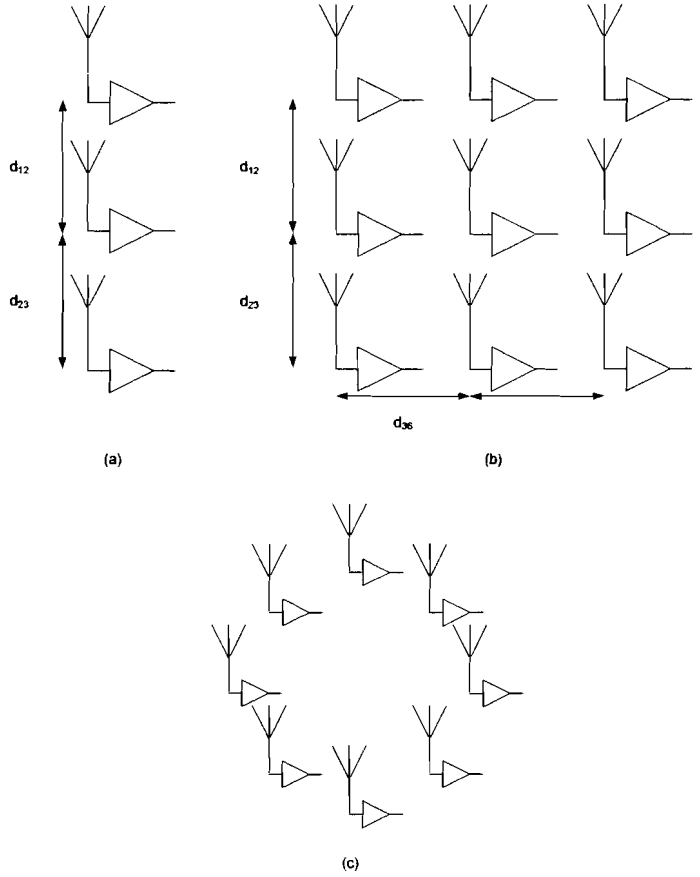

Figure 2.2: Antenna array structure: a) 3 Element linear antenna array; b) 3x3 Element antenna planar; c) Circular antenna array

Key assumptions made with respect to the antenna array are:

1. The incident field is a plane wave.
2. The bandwidth of the modulating signal is small compared to the carrier frequency f_c. This assumption implies that there will be little variation in the modulation over the physical dimensions of the antenna array.
3. There is no mutual coupling between the antenna elements.

The physical distance between the antenna elements imply that a signal received from a certain direction of arrival (DOA) arrives at each antenna at a different time.

Each antenna is followed by a low noise amplifier (LNA), with gain G_a, which adds noise $n_w(t)$, $n_w(t)$ being complex additive white gaussian noise (AWGN) with power spectral density N_0. Let $m_1(t)$ and $m_2(t)$ be two binary streams transmitted using Quadrature Amplitude Modulation (QAM), with

$$\begin{aligned} m_1(t) &= \sum_n a_n p_b(t - nT) \\ m_2(t) &= \sum_n b_n p_b(t - nT) \end{aligned}$$

with a_n, b_n ± 1 and $p_b(t)$ the basic pulse form, chosen such that no inter symbol interference (ISI) exists.

The modulated signal is described by:

$$s(t) = m_1(t)\sqrt{2}\cos 2\pi f_0 t + m_2(t)\sqrt{2}\sin 2\pi f_0 t \tag{2.1}$$

Let the channel characteristic for antenna k, $k = 1 \ldots N_r$, be defined as $h_k(t) = \alpha_k s(t - \delta_k)$, where α_k is gain and δ_k is the delay that occurs during the transmission. Then the received signal at the output of the LNA of antenna k can be described as:

$$\begin{aligned} r_k(t) &= G_a \alpha_k s(t - \delta_k) + n_{w,k}(t) \\ &= G_a \alpha_k [m_1(t - \delta_k)\sqrt{2}\cos 2\pi f_0 (t - \delta_k) \\ &+ m_2(t - \delta_k)\sqrt{2}\sin 2\pi f_0 (t - \delta_k)] + n_{w,k}(t) \end{aligned} \tag{2.2}$$

2.2 RF front-end

The RF front-end comprises the paths from the LNA to the input of the analog-to-digital converter (ADC). The operations performed in the RF front-end are beam steering, linear combining of the received signals and down conversion to baseband. The RF front-end also adds noise to the received signal. However, assuming G_a to be large, the noise contribution of other devices is negligible. [Couch, 2001]

To compensate for the time delay in each receive path k, a beam steering element can be implemented at RF, intermediate frequency (IF)/baseband or by using a delay in the local oscillator (LO) stage as shown in Figure 2.3. The fourth option is digital signal processing (DSP)in baseband. DSP (digital signal processing), although it would increase the flexibility and accuracy of the system, can be ruled out at this moment as it requires an ADC in each receive path boosting the power consumption to an undesired level. [Hajimiri et.al., 2004]

As the accuracy of the beam steering element for a 60 GHz receiver is not clear yet, it is assumed that the delay, ρ_k, of the beam steering element is at least $1/8$ period of the modulation frequency.

$$\rho_k = \frac{p_k T}{M} \tag{2.3}$$

with $M = 2, 3, 4, 5, 6$ or 8 and $p_k = 0, 1, \ldots, M-1$.

For some combining methods it is relevant that a certain weight can be given to a receive path. For that purpose a variable amplifier, with gain g_k, is implemented in each receive path. The beam steering element for receive path k can be defined as:

$$bs_k(t) = g_k r(t - \rho_k) \tag{2.4}$$

For the other three phase shift possibilities it is at this stage not relevant which option will be implemented as long as:

1. The output of the RF front-end is an in-phase (I) and quadrature (Q) baseband signal
2. For each receive path, the combining algorithm can set the phase shift and path weight

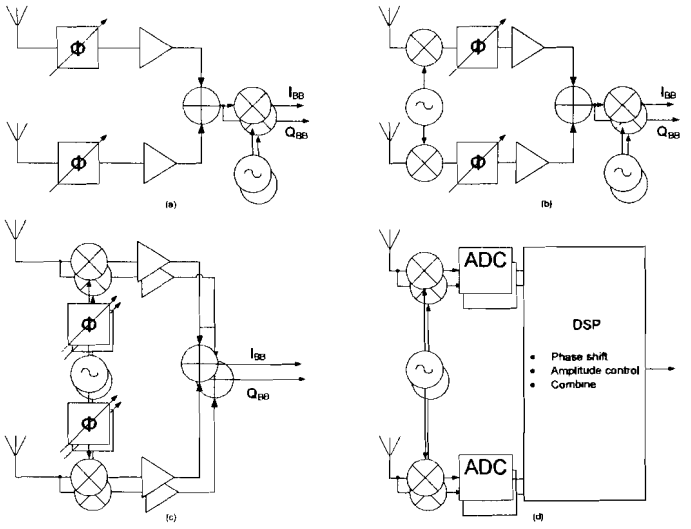

Figure 2.3: Different architectures for implementing phase shift: a) at RF; b) at IF; c) in the LO path; d) Digital phase shift

In this master thesis report, the RF front-end is structured as in Figure 2.2 a. The output of the linear combiner can be described as:

$$\begin{aligned} r_c(t) &= \sum_{k=1}^{N_r} g_k r(t-\rho_k) \\ &= \sum_{k=1}^{N_r} G_a \alpha_k g_k [m_1(t-\delta_k-\rho_k)\sqrt{2}\cos 2\pi f_0(t-\delta_k-\rho_k) \\ &+ m_2(t-\delta_k-\rho_k)\sqrt{2}\sin 2\pi f_0(t-\delta_k-\rho_k)] + g_k n_{w,k}(t) \end{aligned} \tag{2.5}$$

To get the in-phase and quadrature baseband signal, the combined signal $r_c(t)$ is split and multiplied with $\sqrt{2}\cos 2\pi f_0 t$ and $\sqrt{2}\sin 2\pi f_0 t$ respectively.

If this operation is performed on the received signal of Eq.(2.5), where the noise contribution is neglected at this stage, the resulting signals are:

$$\begin{aligned} r_I(t) &= \sum_{k=1}^{N_r} G_a \alpha_k g_k [m_1(t-\delta_k-\rho_k)\{\cos 2\pi f_0(\delta_k+\rho_k) \\ &+ \cos 2\pi f_0(\delta_k+\rho_k)\cos 4\pi f_0 t + \sin 2\pi f_0(\delta_k+\rho_k)\sin 4\pi f_0 t\} \\ &+ m_2(t-\delta_k-\rho_k)\{\cos 2\pi f_0(\delta_k+\rho_k)\sin 4\pi f_0 t - \sin 2\pi f_0(\delta_k+\rho_k) \\ &- \sin 2\pi f_0(\delta_k+\rho_k)\cos 4\pi f_0 t\}] \end{aligned} \tag{2.6}$$

$$\begin{aligned} r_Q(t) &= \sum_{k=1}^{N_r} G_a \alpha_k g_k [m_1(t-\delta_k-\rho_k)\{\cos 2\pi f_0(\delta_k+\rho_k)\sin 4\pi f_0 t \\ &+ \sin 2\pi f_0(\delta_k+\rho_k) + \sin 2\pi f_0(\delta_k+\rho_k)\sin 4\pi f_0 t\} \\ &+ m_2(t-\delta_k-\rho_k)\{\cos 2\pi f_0(\delta_k+\rho_k) + \cos 2\pi f_0(\delta_k+\rho_k)\sin 4\pi f_0 t \\ &- \sin 2\pi f_0(\delta_k+\rho_k)\sin 4\pi f_0 t\}] \end{aligned} \tag{2.7}$$

Assuming $m_i(t-\delta_k-\rho_k) \cong m_i(t)$, the in-phase and quadrature output after low-pass filtering equals:

$$\begin{aligned} r_I(t) &= \sum_{k=1}^{N_r} G_a \alpha_k g_k [m_1(t)\cos 2\pi f_0(\delta_k+\rho_k) - m_2(t)\sin 2\pi f_0(\delta_k+\rho_k)] \\ r_Q(t) &= \sum_{k=1}^{N_r} G_a \alpha_k g_k [m_1(t)\sin 2\pi f_0(\delta_k+\rho_k) - m_2(t)\cos 2\pi f_0(\delta_k+\rho_k)] \end{aligned} \tag{2.8}$$

2.3 Analog-to-Digital conversion

The RF front-end output is followed by two, one for the in-phase output and one for the quadrature output of the RF front-end, analog-to-digital converters. The incoming I and Q baseband signals are sampled and quantized. The sampling rate and the number of quantization levels are an indication of the accuracy of the digital signal, hence the level of quantization noise. In chapter 6 the effect of analog-to-digital conversion will be simulated and evaluated.

2.4 Receiver logic

The output of the ADCs are connected to both the baseband processor and the receiver logic. In a pre-defined time period, a number of training symbols are sent, this is possible in the preamble or in a postamble. The receiver logic can perform its combining algorithm and set the phase shift and weight for each receive path. This operation is described in the following chapters of this thesis.

2.5 Equivalent complex baseband model

Given the modulated signal of Eq. (2.1), $s(t)$ may be rewritten to:

$$s(t) = s_I \cos 2\pi f_0 t + s_Q \sin 2\pi f_0 t \tag{2.9}$$

with $s_I(t) = \sqrt{2}m_1(t)$ and $s_Q(t) = -\sqrt{2}m_2(t)$.

The complex envelope of signal $s(t)$ is defined as:

$$\tilde{s}(t) = s_I(t) + i\, s_Q(t) \tag{2.10}$$

Using Euler's formula, $e^{i2\pi f_0(t)} = \cos 2\pi f_0(t) + i \sin 2\pi f_0(t)$, $s(t)$ and $\tilde{s}(t)$ are related by:

$$s(t) = Re\{\tilde{s}(t)e^{i2\pi f_0(t)}\} \tag{2.11}$$

The complex envelope $\tilde{s}(t)$ completely preserves the information content of the modulated signal $s(t)$ except for the carrier frequency f_0.

The delayed, attenuated received signal with AWGN at antenna k, $r_k(t)$, from Eq. (2.2) can be expressed in a complex envelope notation according to:

$$\tilde{r}(t) = G_a \alpha_k \tilde{s}(t)e^{i2\pi f_0 \delta_k} + \tilde{n}_{w,k}(t) \tag{2.12}$$

with $\tilde{n}_{w,k}(t)$ the complex envelope representation of $n_{w,k}(t)$. Both the in-phase as quadrature components of $n_{w,k}(t)$ are AWGN and independent of each other. The corresponding complex baseband process $\tilde{n}_{w,k}(t)$ has a two sided noise spectral density of N_0.

Finally, the combined complex envelope of the received signal after beam steering and low-pass filtering is defined as:

$$\begin{aligned} \tilde{r}_c(t) &= \sum_{k=1}^{N_r} G_a \alpha_k g_k \tilde{s}(t)e^{i2\pi f_0(\delta_k+\rho_k)} + g_k \tilde{n}_{w,k}(t)e^{i2\pi f_0 \rho_k} \\ &= \sum_{k=1}^{N_r} G_a \alpha_k g_k \tilde{s}(t)e^{i2\pi f_0(\delta_k+\rho_k)} + g_k \tilde{n}_{w,k}(t) \end{aligned} \tag{2.13}$$

As the noise process is circular symmetrical, delay does not influence this process.

Let θ_k and ϕ_k be defined as

$$\begin{aligned} \theta_k &= 2\pi f_0 \delta_k \\ \phi_k &= 2\pi f_0 \rho_k \end{aligned}$$

Eq. (2.13) may be rewritten as:

$$\tilde{r}_c(t) = \sum_{k=1}^{N_r} G_a \alpha_k g_k \tilde{s}(t)e^{i(\theta_k+\phi_k)} + g_k \tilde{n}_{w,k}(t) \tag{2.14}$$

Analog-to-digital conversion is performed using the real and imaginary part of $\tilde{r}_c(t)$. [Haykin and Moher, 2005]

Chapter 3

Beamforming techniques

Beamforming, a name derived from directional antennas designed to form a pencil beam radiation pattern, is a process of spatial filtering which can be implemented at both transmitter and receiver. In general a beamformer performs spatial filtering of signals with overlapping frequency content but originating from different spatial locations.

Beamformers, in general, require knowledge of the direction of arrival (DOA) of the desired signal or the time delay caused by the DOA and transmit channel characteristics. These parameters are usually not known, but can be estimated from the available data. Parameters may also change over time. To solve these problems, the parameters are determined by an adaptive beamforming algorithm. Adaptive algorithms can be divided into two basic approaches: block adaption and continuous adaption. Block adaption estimates the required parameters from a temporal block of array data, where the continuous adaption adjusts the parameters while receiving data such that these converges to the optimum solution.

Implementation of an adaptive beamforming algorithm in a wireless data communication system implies the use of a block adaption approach. Changes in the receiver settings during the reception of the data block may cause undesired effects and therefore introducing bit errors. The common known wireless standards already apply some block adaptive processes, like frequency fine tuning and automatic gain control. These processes are executed during a preamble, sent before the data block. If a beamforming algorithm will be implemented into a wireless communication standard, the preamble might be the place where adaptive beamforming will be performed.[Tanenbaum, 2003]

In this chapter some basic terminology will be described followed by possible adaptive beamforming solutions. This will be used to develop beamforming algorithms in the following chapters. [van Veen and Buckley, 1988]

3.1 Basic terminology

In this chapter some terminology and concepts are introduced. These form a basis for the next sections in which possible beamforming solutions are presented.

3.1.1 Phased array versus delayed array

A wavefront arriving at an antenna array under a direction of arrival (DOA) introduces a time delay in arrival at each individual antenna. This time delay between two adjacent antennas, ΔT depends on the DOA and the antenna spacing according to

$$d \sin(DOA) = c\Delta T \tag{3.1}$$

with the distance between the antennas,d and the speed of light, c.

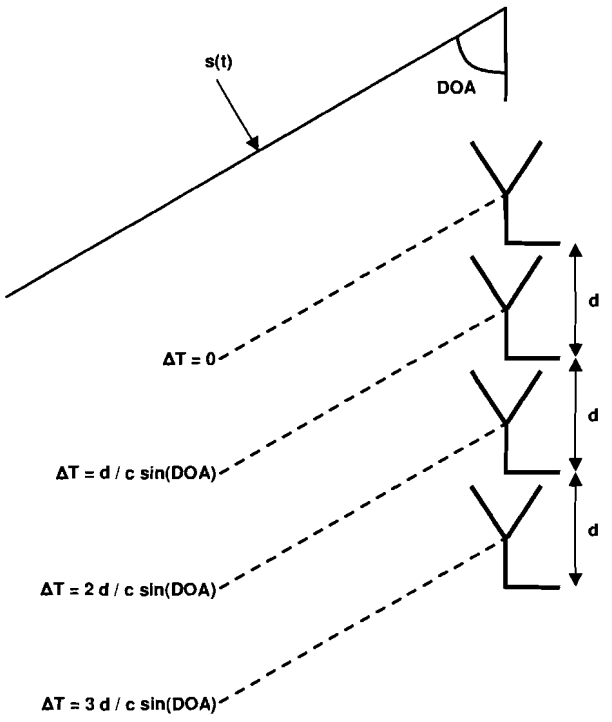

Figure 3.1: Relation between DOA and time delay for linear antenna array

Beamforming is a method of compensating the time delay for each antenna by implementing an ideal delay element in each receive path. However, these ideal delay elements are difficult to implement. A more practical solution is to translate the time difference into a phase shift in the frequency domain. If the

desired signal consists of a single frequency, time delay between two adjacent antennas can be replaced by a phase shift, Δp using

$$\begin{aligned} \Delta p &= 2\pi \, \Delta T \, f_0 \\ &= 2\pi \, \frac{d}{c} \sin(DOA) \, f_0 \\ &= 2\pi \, \frac{d}{\lambda} \sin(DOA) \end{aligned} \tag{3.2}$$

Eq. (3.2) calculates the phase shift for a signal using a single frequency. If the desired signal consists of a larger bandwidth, using Eq. (3.2) introduces a phase distortion. As long as the signal bandwidth is small compared to the carrier frequency, this distortion remains limited.

Example 3.1: Using an antenna array with $d = \lambda/4$, the phase distortion of a signal with center carrier frequency $f_0 = 60GHz$ and bandwidth 1 Ghz, gets a phase distortion, for $\Delta T = 4.1667 \cdot 10^{-12}$ (which equals a DOA of 90 degrees at 60 GHz) can be calculated as follows:
$f = 60$ GHz:

$$\begin{aligned} \Delta p &= 2\pi \, 4.1667 \cdot 10^{-12} \, 60 \cdot 10^9 \\ &= 1.5708 \end{aligned}$$

$f = 59.5$ GHz:

$$\begin{aligned} \Delta p &= 2\pi \, 4.1667 \cdot 10^{-12} \, 59.5 \cdot 10^9 \\ &= 1.5577 \end{aligned}$$

$f = 60.5$ GHz:

$$\begin{aligned} \Delta p &= 2\pi \, 4.1667 \cdot 10^{-12} \, 60.5 \cdot 10^9 \\ &= 1.5839 \end{aligned}$$

A phase distortion of $\pm 0.0131 rad$

In chapter 2 it is already assumed that the signal bandwidth is small compared to the carrier frequency. For further beamforming implementation the phased antenna array will be used.

3.1.2 Signal representation

Using the relationship between DOA and antenna spacing as described in the previous part, a representation of the received signal can be derived. Eq. (2.14) gives the complex envelope of the received baseband signal. In this equation θ_k is the phase shift caused by the time delay of the received signal at antenna

k. If signal $r_k(t)$ is the received signal at antenna k under DOA β, θ_k can be expressed as:

$$\theta_k = \theta_1 + (k-1)2\pi\frac{d\sin(\beta)}{\lambda} \tag{3.3}$$

3.2 Block adaptive beamforming

Block adaptive beamforming may be used in a non-stationary environment, provided the statistics are recomputed periodically. In a wireless data communication system, a data packet usually is provided with a preamble during which the necessary statistics can be estimated. Given the general receiver architecture two possible adaptive beamforming algorithms may be used:

1. Maximization of signal-to-noise ratio beamforming
2. Power controlled beamforming

Maximization of SNR beamforming requires knowledge of the statistics, defined by the channel transfer matrix and phase shift caused by the DOA. Reference signal beamforming sets the beam direction based on the maximum received training symbol power.

3.2.1 Maximization of signal-to-noise ratio beamforming

Maximization of SNR beamforming uses the channel estimation to set phase and weight for each antenna branch such that the SNR is maximized. Known combining techniques for this beamforming algorithm are:

1. Maximal-ratio combining
2. Equal-gain combining

Maximal-ratio combining

The maximal-ratio combiner consists of N_r linear receivers, followed by a linear combiner. Each receive path, k, consists of an antenna, a low noise amplifier with variable gain G_a and a beam steering element with gain g_k and phase shift ϕ_k. The combination of g_k and ϕ_k will further be referred to as the complex weighting factor a_k with $a_k = g_k e^{i\phi_k}$. Unless stated otherwise it is assumed that $G_a = 1$. The complex envelope of the received signal at the output of the LNA of the k^{th} receive branch is defined as [Haykin and Moher, 2005]:

$$\tilde{r}_k(t) = \alpha_k \tilde{s}(t) e^{i\theta_k} + \tilde{n}_{w,k}(t) \tag{3.4}$$

The complex envelope of the output of the linear combiner is defined by:

$$\tilde{r}_c(t) = \sum_{k=1}^{N_r} \alpha_k a_k \tilde{s}(t) e^{i\theta_k} + a_k \tilde{n}_{w,k}(t) \tag{3.5}$$

Under assumption that the $n_{w,k}(t)$ are mutually independent for $k = 1, 2, \ldots, N_r$, the output signal-to-noise ratio is

$$\begin{aligned} SNR &= \frac{\mathbf{E}[|\tilde{s}(t) \sum_{k=1}^{N_r} \alpha_k a_k e^{i\theta_k}|^2]}{\mathbf{E}[|\sum_{k=1}^{N_r} a_k \tilde{n}_{w,k}(t)|^2]} \\ &= \frac{\mathbf{E}[|\tilde{s}(t)|^2]}{\mathbf{E}[|\tilde{n}_{w,k}(t)|^2]} \cdot \frac{\mathbf{E}[|\sum_{k=1}^{N_r} \alpha_k a_k e^{i\theta_k}|^2]}{\mathbf{E}[\sum_{k=1}^{N_r} |a_k|^2]} \\ &= (\frac{E}{N_0}) \frac{\mathbf{E}[|\sum_{k=1}^{N_r} \alpha_k a_k e^{i\theta_k}|^2]}{\mathbf{E}[\sum_{k=1}^{N_r} |a_k|^2]} \end{aligned} \tag{3.6}$$

Using

$$|\sum_{k=1}^{N_r} \alpha_k a_k e^{i\theta_k}|^2 \text{ and } \sum_{k=1}^{N_r} |a_k|^2$$

as the instantaneous values of the expectations in the numerator and denominator of Eq. (3.6) respectively, the instantaneous output signal-to-noise ratio, γ, equals

$$\gamma = (\frac{E}{N_0}) \frac{|\sum_{k=1}^{N_r} \alpha_k a_k e^{i\theta_k}|^2}{\sum_{k=1}^{N_r} |a_k|^2} \tag{3.7}$$

To obtain the maximum signal-to-noise ratio, it is required to maximize γ with respect to a_k. This can either be done by the standard differentiation method, or by using the Cauchy-Schwarz inequality

$$|\sum_{k=1}^{N_r} a_k b_k|^2 \leq \sum_{k=1}^{N_r} |a_k|^2 \sum_{k=1}^{N_r} |b_k|^2 \tag{3.8}$$

applying this inequality to Eq.(3.7) with $b_k = \alpha_k e^{j\theta_k}$ we obtain

$$\gamma \leq (\frac{E}{N_0}) \frac{\sum_{k=1}^{N_r} |a_k|^2 \sum_{k=1}^{N_r} |\alpha_k e^{i\theta_k}|^2}{\sum_{k=1}^{N_r} |a_k|^2} \tag{3.9}$$

canceling common terms results in

$$\gamma \leq (\frac{E}{N_0}) \sum_{k=1}^{N_r} \alpha_k^2 \tag{3.10}$$

The inequality of Eq.(3.9) holds with equality for

$$\begin{aligned} a_k &= c(\alpha_k e^{i\theta_k})^* \\ &= c\alpha_k e^{-i\theta_k} \end{aligned} \tag{3.11}$$

where c is some arbitrary complex constant and $k = 1, 2, \ldots, N_r$. Hence, the instantaneous output signal-to-noise ratio of the maximal-ratio combiner is

$$\gamma = (\frac{E}{N_0}) \sum_{k=1}^{N_r} \alpha_k^2 \tag{3.12}$$

Equal-gain combining

Equal-gain combining (EGC) is similar to maximal-ratio combining except the fact that for a_k, as in Eq. (3.11), all α_k's are set to 1. Examining Eq. (3.9) shows that the instantaneous SNR is unchanged, hence in the ideal case the use of EGC is preferred over the use of MRC for its smaller complexity. However, if $a_k \neq c(\alpha_k e^{i\theta_k})^*$, Eq.(3.12) does not hold. Instead Eq. (3.7) should be used, which shows that EGC does not achieve the same SNR as MRC. The use of EGC, therefore, should be evaluated for each case in which MRC is used. Performance loss is to be expected, however could be compensated by a less complex architecture.

3.2.2 Power controlled beamforming

Power controlled beamforming uses the received power to estimate the direction in which the beam needs to be set. Power controlled beamforming uses a number of training symbols in a pre-defined time period. For each training symbol the beam is set in a different direction. On reception of the training symbol, the average received power is determined. Finally, the beamforming algorithm can set the phase shift in the receive paths such that the received power is maximized. For this algorithm, channel characteristics and DOA need not be known, reducing the algorithm complexity and resulting in less processing time and memory requirements.

The output of the receiver, as in Eq.(3.5), is

$$\tilde{r}_c(t) = \sum_{k=1}^{N_r} \alpha_k a_k \tilde{s}(t) e^{i\theta_k} + a_k \tilde{n}_{w,k}(t) \tag{3.13}$$

The settings for the phases shifters in the receive paths are optimum if the average received power is maximal. The average received power is calculated by:

$$P_{av} = \mathbf{E}[\tilde{r}_c(t) \cdot \tilde{r}_c(t)^*] \tag{3.14}$$

Chapter 4

Maximization of SNR beamforming

Maximization of signal-to-noise ratio beamforming, as described in Chapter 3, requires channel estimation followed by a combining method. Maximal-ratio combining will result in an optimum signal-to-noise ratio at the output of the receiver. MRC requires a beam steering element in each receive path, with complex weighting factor a_k as shown in Eq.(3.11), capable of exactly compensating the receive path statistics except for a common factor for all receive paths. The beam steering elements, as described in Chapter 2, however, are not capable of setting the weighting factor in such way that this requirement is met. This chapter shows the loss in performance due to this limitation. The major challenge of this master thesis is to develope beamforming algorithms capable of minimizing this loss (approaching the maximal SNR at the output of the receiver equal to the MRC result). In this chapter channel estimation and two combining methods, based upon MRC, are described. The second combining algorithm achieves an optimum result given the limitations of the beam steering element.

4.1 Channel estimation

Channel estimation for the given receiver architecture is needed to estimate gain and phase angle for each receive path. This information is required for the beamforming algorithm to find the settings for weight and phase shifters to achieve maximum SNR at the output of the receiver. The output of the receiver is the combined baseband signal, hence a technique is required to distinguish between the different receive paths. Such a method uses a series of training symbols, each symbol long enough to minimize the effects of noise.

4.1.1 Training symbols

Provided channel characteristics do not change during the period in which the training is sent and over the bandwidth used, channel estimation can be performed and the results can be used to set phase shift and weight in the receive paths.

The number of samples of the training symbol is of importance to minimize the effect of noise. The more samples the more accurate the channel estimation becomes. Figure 4.1 shows the probability density function for the estimation of the channel gain using a training symbol, with 50, 100, 500 and 1000 samples respectively. The estimation is performed using a SNR of 0 dB and channel gain 1.

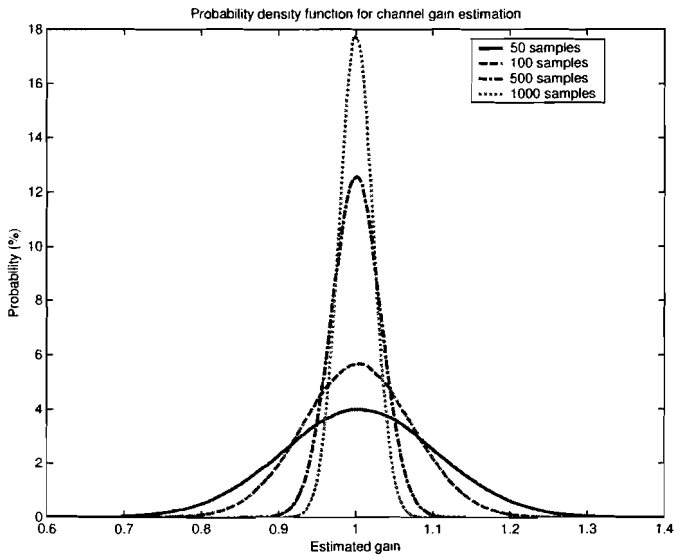

Figure 4.1: Probability density function for channel gain estimation

Define T_n as the complex envelope of the n^{th} training symbol T and $\alpha_k T_n e^{i\theta_k}$ as the complex envelope of the received training symbol at antenna k under a certain DOA.

4.1.2 Full channel estimation

Individual channel estimation

The easiest way to perform a channel estimation for N_r receive paths is to send N_r training symbols and determine the received symbol for one receive path at a time. During each training symbol, all receive paths are switched off except

for one. Let subscript n of $T_n(t)$ describe which receive path is not switched off. The output of the receiver can be described as:

$$\tilde{r}_n = \alpha_n T_n e^{i\theta_n} \tag{4.1}$$

with α_n the channel gain for receive path n.

If this operation is performed for $n = 1 \ldots N_r$, phase shift θ_k and channel gain α_k can be estimated for $k = 1 \ldots N_r$.

Walsh-Hadamard matrix estimation

If, for technical reasons, receive paths cannot be switched off, individual channel estimation cannot be performed. An alternative method uses an orthogonal linear combination of all received training symbols. An orthogonal linear combination can be based on a Walsh-Hadamard matrix. This matrix is defined as:

$$H_1 = \begin{pmatrix} 1 \end{pmatrix}$$

and

$$H_n = \frac{1}{\sqrt{2}} \begin{pmatrix} H_{n/2} & H_{n/2} \\ H_{n/2} & -H_{n/2} \end{pmatrix}$$

In practice this means that two operations need to be performed. Firstly a combination of the received training symbol n according to the n^{th} row of the Walsh-Hadamard matrix, where the sign of the k^{th} element in the row stands for the sign of the k^{th} receive path. The received n^{th} training symbol at antenna k is defined as $\tilde{r}_{n,k}$. With $\tilde{r}_{n,k} = \alpha_k g_k T_n e^{i\theta_k}$.

g_k is set to $\frac{1}{\sqrt{N_r}}$ for all k.

Example 4.1: For a receiver with 4 receive paths the Walsh-Hadamard matrix is:

$$H_4 = \frac{1}{\sqrt{4}} \begin{pmatrix} 1 & 1 & 1 & 1 \\ 1 & -1 & 1 & -1 \\ 1 & 1 & -1 & -1 \\ 1 & -1 & -1 & 1 \end{pmatrix}$$

The combined output of the receiver, $\tilde{r}_{c,n}$ for $n = 1 \ldots 4$, with $g_k = \frac{1}{\sqrt{4}}$ is:

$$\begin{aligned}
\tilde{r}_{c,1} &= \frac{1}{\sqrt{4}}[\tilde{r}_{1,1} + \tilde{r}_{1,2} + \tilde{r}_{1,3} + \tilde{r}_{1,4}] \\
\tilde{r}_{c,2} &= \frac{1}{\sqrt{4}}[\tilde{r}_{2,1} - \tilde{r}_{2,2} + \tilde{r}_{2,3} - \tilde{r}_{2,4}] \\
\tilde{r}_{c,3} &= \frac{1}{\sqrt{4}}[\tilde{r}_{3,1} + \tilde{r}_{3,2} - \tilde{r}_{3,3} - \tilde{r}_{3,4}] \\
\tilde{r}_{c,4} &= \frac{1}{\sqrt{4}}[\tilde{r}_{4,1} - \tilde{r}_{4,2} - \tilde{r}_{4,3} + \tilde{r}_{4,4}]
\end{aligned}$$

Secondly RT_k, $k = 1 \ldots N_r$, can be calculated by combining $\tilde{r}_{c,1}$ to $\tilde{r}_{c,N_r}$ according to the k^{th} row of the Walsh-Hadamard matrix and multiplying this result with $\frac{1}{\sqrt{N_r}}$.

Example 4.2: Given $\tilde{r}_{c,1}$ to $\tilde{r}_{c,4}$ of example 4.1, RT_1 to RT_n can be calculated as follows:

$$\begin{aligned}
RT_1 &= \frac{1}{\sqrt{4}}[\tilde{r}_{c,1} + \tilde{r}_{c,2} + \tilde{r}_{c,3} + \tilde{r}_{c,4}] \\
RT_2 &= \frac{1}{\sqrt{4}}[\tilde{r}_{c,1} - \tilde{r}_{c,2} + \tilde{r}_{c,3} - \tilde{r}_{c,4}] \\
RT_3 &= \frac{1}{\sqrt{4}}[\tilde{r}_{c,1} + \tilde{r}_{c,2} - \tilde{r}_{c,3} - \tilde{r}_{c,4}] \\
RT_4 &= \frac{1}{\sqrt{4}}[\tilde{r}_{c,1} - \tilde{r}_{c,2} - \tilde{r}_{c,3} + \tilde{r}_{c,4}]
\end{aligned}$$

resulting in:

$$\begin{aligned}
RT_1 &= \alpha_1 T\, e^{i\theta_1} \\
RT_2 &= \alpha_2 T\, e^{i\theta_2} \\
RT_3 &= \alpha_3 T\, e^{i\theta_3} \\
RT_4 &= \alpha_4 T\, e^{i\theta_4}
\end{aligned}$$

Using RT_1 to RT_{N_r}, θ_k and α_k can be estimated for $k = 1 \ldots N_r$.

4.1.3 Partial channel estimation

The drawback of a full channel estimation is that for estimating N_r antennas an equal amount of training symbols need to be sent. If N_r grows, the amount of training symbols grows linearly. Using the knowledge that the phase of the signal received at antenna k, compared to the phases of the signals received at the other antennas, depends on the DOA of the signal, the phases for all received signals can be estimated when only the phase difference between two

received signals is known. If the phase difference between two adjacent receive paths is estimated, the phases for all received signals can be estimated. If θ_1 and θ_2 are estimated, the phase difference p can be defined as $p = \theta_2 - \theta_1$. The phases for the other receive antennas can be calculated using the following relation: $\theta_k = \theta_2 + (k-2)p$. A more accurate estimation can be achieved if more phases are estimated and P is defined as the average of all found p's.

4.2 Combining methods

4.2.1 Rounding method

The first combination algorithm is based upon MRC. The algorithm uses the information provided by the channel estimation. This information is used to set the weight in the receive path. Secondly the channel estimation is used to set the phase shifter in the receive path in such a way that the phase of the received signal is as small as possible. To achieve this, the phase will be rounded to the nearest possible phase shift.

Method

Provided the Walsh-Hadamard channel estimation has been performed, the rounding algorithm uses the results to set $g_1 \dots g_{N_r}$. Consequently the estimated channel phase θ_k will be used to set ϕ_k, with

$$\phi_k = min|\theta_k - \frac{2p_k\pi}{M}| \; with\, p_k = 0, 1, \dots, M-1 \tag{4.2}$$

Performance

Eq.(3.12) gives an upper bound for the SNR using MRC. Given the limitations of the phase shift in the receiver, this phase shift, ϕ_k, can be set in M values, $\phi_k = 2p_k\pi/M$ with $p_k = 0, 1, \dots, M-1$. Assume the receiver logic rounds the estimated phase angle in receive path k, θ_k, to the nearest possible phase shift angle ϕ_k. The phase angle after compensation, φ_k, is defined by

$$\varphi_k = \theta_k - \phi_k \tag{4.3}$$

and is limited by $\pm\,\pi/M$.

If $\varphi_k = c$ for all $k = 1 \dots N_r$, with c an arbitrary complex constant, the rounding method achieves this upper bound.
However, if $\varphi_k \neq c$ for all $k = 1 \dots N_r$, Eq.(3.12) does not hold. For the

signal-to-noise ratio achieved by the combining algorithm we will use Eq.(3.7) instead. Using the definition of a_k the instantaneous signal-to-noise ratio of Eq.(3.7) equals

$$\begin{aligned}
\gamma &= (\frac{E}{N_0})\frac{|\sum_{k=1}^{Nr} a_k\alpha_k e^{i\theta_k}|^2}{\sum_{k=1}^{Nr}|a_k|^2} \\
&= (\frac{E}{N_0})\frac{|\sum_{k=1}^{Nr} g_k\alpha_k e^{-i\phi_k}e^{i\theta_k}|^2}{\sum_{k=1}^{Nr}|g_k e^{-i\phi_k}|^2} \qquad (4.4)\\
&= (\frac{E}{N_0})\frac{|\sum_{k=1}^{Nr} \alpha_k^2 e^{i(\theta_k-\phi_k)}|^2}{\sum_{k=1}^{Nr}\alpha_k^2}
\end{aligned}$$

A lower bound for Eq.(4.6) can be found by minimizing $|\sum_{k=1}^{Nr}\alpha_k^2 e^{i(\theta_k-\phi_k)}|^2$

$$\begin{aligned}
\mu &= min(|\sum_{k=1}^{Nr}\alpha_k^2 e^{i(\theta_k-\phi_k)}|^2) \\
&= min(|\sum_{k=1}^{N_r}\alpha_k^2 e^{i\varphi_k}|^2) \\
&= min(|\sum_{k=1}^{N_r}\alpha_k^2[\cos(\varphi_k)+i\sin(\varphi_k)]|^2) \qquad (4.5)\\
&= min(|\sum_{k=1}^{N_r}\alpha_k^2\cos(\varphi_k)+i\sum_{k=1}^{N_r}\alpha_k^2\sin(\varphi_k)|^2)
\end{aligned}$$

The minimum for Eq.(4.7) can be found if $\varphi_k \rightarrow \pm\pi/2$, if applicable bounded by $\pm\pi/M$, $\varphi_k = -\varphi_{N_r-k+1}$ and $\alpha_1 = \alpha_2 = \ldots = \alpha_{N_r}$.

Example 4.3: Lower bound
$N_r = 2$, $M = 8$, $\alpha_k = 1$ for all k
$M = 8 \Rightarrow |\varphi_k|_{max} = \pi/8$
Assume $\varphi_1 = \pi/8$ and $\varphi_2 = -\pi/8$

$$\gamma = (\frac{E}{N_0})\frac{|\sum_{k=1}^{N_r} e^{i(\theta_k-\phi_k)}|^2}{2}$$

$$
\begin{aligned}
&= (\frac{E}{N_0})\frac{|\sum_{k=1}^{N_r} \cos(\varphi_k) + i\sin(\varphi_k)|^2}{2} \\
&= (\frac{E}{N_0})\frac{|(\cos(\pi/8) + i\sin(\pi/8)) + (\cos(-\pi/8) + i\sin(-\pi/8))|^2}{2} \\
&= (\frac{E}{N_0})\frac{|2\cos(\pi/8)|^2}{2} \\
&= (\frac{E}{N_0})2\cos^2(\pi/8)
\end{aligned}
$$

if you compare this to the upper bound found in Eq.(3.12), this is a factor $\cos^2(\pi/M)$ smaller.

4.2.2 Optimized rounding method

Although the above described algorithm achieves the smallest phase per receive branch after compensation, this does not, in all cases, implies an optimum SNR at the output. Example 4.4 will show a situation in which a larger phase angle after compensation will result in a better performance of the combining algorithm.

Example 4.4: Non-optimum result
$N_r = 2$, $M = 8$, $\alpha_k = 1$ for all k
Assume $\varphi_1 = \pi/8$ and $\varphi_2 = -\pi/10$

$$
\begin{aligned}
\gamma &= (\frac{E}{N_0})\frac{|\sum_{k=1}^{N_r} e^{i\varphi_k}|^2}{2} \\
&= (\frac{E}{N_0})\frac{|\sum_{k=1}^{N_r} \cos(\varphi_k) + i\sin(\varphi_k)|^2}{2} \\
&= (\frac{E}{N_0})\frac{|(\cos(\pi/8) + i\sin(\pi/8)) + (\cos(-\pi/10) + i\sin(-\pi/10))|^2}{2} \\
&= (\frac{E}{N_0})\frac{|\cos(\pi/8) + \cos(-\pi/10) + i(\sin(\pi/8) + \sin(-\pi/10))|^2}{2} \\
&= (\frac{E}{N_0})\frac{|1.87494 + j(0.07367))|^2}{2} \\
&= (\frac{E}{N_0})1.7604
\end{aligned}
$$

Let φ_2 be $\varphi_2 + \pi/4 = 3\pi/20$

$$
\gamma = (\frac{E}{N_0})\frac{|\sum_{k=1}^{N_r} e^{i\varphi_k}|^2}{2}
$$

$$
\begin{aligned}
&= (\frac{E}{N_0})\frac{|\sum_{k=1}^{N_r} \cos(\varphi_k) + i\sin(\varphi_k)|^2}{2} \\
&= (\frac{E}{N_0})\frac{|(\cos(\pi/8) + i\sin(\pi/8)) + (\cos(3\pi/20) + i\sin(3\pi/20))|^2}{2} \\
&= (\frac{E}{N_0})\frac{|\cos(\pi/8) + \cos(3\pi/20) + i(sin(\pi/8) + \sin(3\pi/20))|^2}{2} \\
&= (\frac{E}{N_0})\frac{|1.81489 + j(0.83667))|^2}{2} \\
&= (\frac{E}{N_0})1.9969
\end{aligned}
$$

A gain of 1.1 dB compared to the rounding algorithm.

An explanation for this result lies in the fact that the result of the summation $|\sum_{k=1}^{N_r} \alpha_k^2 e^{j\varphi_k}|^2$ depends on the difference between the φ_k's. Rewriting this summation shows

$$
\begin{aligned}
& |\sum_{k=1}^{N_r} \alpha_k^2 e^{j\varphi_k}|^2 \\
&= |\sum_{k=1}^{N_r} \alpha_k^2[\cos(\theta_k - \phi_k) + i\sin(\theta_k - \phi_k)]|^2 \qquad (4.6) \\
&= \sum_{k=1}^{N_r} \alpha_k^4 + \sum_{k=1}^{N_r-1}\sum_{l=k+1}^{N_r} 2\alpha_k^2\alpha_l^2 \cos((\theta_k - \phi_k) - (\theta_l - \phi_l))
\end{aligned}
$$

Using ϕ as the only degree of freedom, the following algorithm results in an optimum SNR at the output of the receiver.

Method

Use the rounding algorithm to set g_k and ϕ_k of the beam steering elements. Calculate the output for the rounding algorithm and keep this as initial result. Sort φ_k in descending order, for $k = 1 \ldots N_r$, such that $\varphi'_1 \geq \varphi'_2 \geq \ldots \geq \varphi'_{N_r}$. If $\varphi'_1 - \varphi'_{N_r} \leq \pi/M$, the rounding method is optimal and no optimization is needed.
If $\varphi_1 - \varphi_{N_r} > \pi/M$, change φ'_1 into $\varphi'_1 - 2\pi/M$ and calculate the SNR at the output of the receiver. Repeat this step for $k = 2 \ldots N_r - 1$. The maximum of the calculated SNR and initial SNR is the maximum achievable SNR at the output of the receiver. Apply the settings for ϕ_k, $k = 1 \ldots N_r$, according to the settings for which the output is maximal.

Performance

This paragraph proofs that the optimized rounding algorithm finds the maximal SNR at the output of the receiver.

Assume:

1. $\Phi = 2\pi/M$
2. $\varphi'_1 \geq \varphi'_2 \geq \ldots \geq \varphi'_{N_r}$
3. $\Phi \leq \frac{\pi}{2}$
4. SNR_x is the SNR at the output of the receiver when φ'_k is set to $\varphi'_k - \Phi$, for $k = 1 \ldots x$
5. $SNRr_x$ is the SNR at the output of the receiver when φ'_k is set to $\varphi'_k + \Phi$, for $k = N_r, N_r - 1, \ldots, x$

The SNR at the output of the receiver is maximal for

$$\begin{aligned} & max(|\sum_{k=1}^{N_r} \alpha_k^2[\cos(\varphi_k) + i\sin(\varphi_k)]|^2) \\ = \; & max(\sum_{k=1}^{N_r} \alpha_k^4 + \sum_{k=1}^{N_r-1}\sum_{l=k+1}^{N_r} 2\alpha_k^2\alpha_l^2\cos(\varphi_k - \varphi_l)) \\ = \; & arg(max(\sum_{k=1}^{N_r-1}\sum_{l=k+1}^{N_r} 2\alpha_k^2\alpha_l^2\cos(\varphi_k - \varphi_l))) \end{aligned} \tag{4.7}$$

Lemma 4.1: If changing φ'_k into $\varphi'_k - \Phi$, for $k = 1 \ldots N$ implies $SNR_N \geq SNR_M$, $M < N$. Changing $\varphi_l - \Phi$ back to φ_l, for $l < N$ implies the SNR at the output of the receiver to be less or equal than SNR_N.

Change φ'_k into $\varphi'_k - \Phi$, for $k = 1 \ldots N$

Changing φ_k into $\varphi_k - \Phi$ for $k = 1 \ldots N$ results in Eq. (4.9) to become:

$$\begin{aligned} & \sum_{k=1}^{N-1}\sum_{l=k+1}^{N} 2\alpha_k^2\alpha_l^2\cos(\varphi_k - \varphi_l) + \sum_{k=1}^{N-1}\sum_{l=N+1}^{N_r} 2\alpha_k^2\alpha_l^2\cos((\varphi_k - \Phi) - \varphi_l) \\ + \; & \sum_{k=N}^{N_r-1}\sum_{l=k+1}^{N_r} 2\alpha_k^2\alpha_l^2\cos(\varphi_k - \varphi_l) \end{aligned} \tag{4.8}$$

Change φ'_k into $\varphi'_k - \Phi$, for $k = 1 \ldots N-1$

Changing φ_k into $\varphi_k - \Phi$ for $k = 1 \ldots N-1$ results in Eq. (4.9) to become:

$$\sum_{k=1}^{N-2}\sum_{l=k+1}^{N-1} 2\alpha_k^2\alpha_l^2\cos(\varphi_k - \varphi_l) + \sum_{k=1}^{N-2}\sum_{l=N}^{N_r} 2\alpha_k^2\alpha_l^2\cos((\varphi_k - \Phi) - \varphi_l) + \sum_{k=N-1}^{N_r-1}\sum_{l=k+1}^{N_r} 2\alpha_k^2\alpha_l^2\cos(\varphi_k - \varphi_l) \tag{4.9}$$

$SNR_N \geq SNR_{N-1}$ implies Eq.(4.10) $\geq$ Eq.(4.11), which yields:

$$\sum_{k=1}^{N-1} 2\alpha_k^2\alpha_N^2\cos(\varphi_k - \varphi_N) + \sum_{l=N+1}^{N_r} 2\alpha_N^2\alpha_l^2\cos((\varphi_N - \Phi) - \varphi_l)$$

$$\geq$$

$$\sum_{k=1}^{N-1} 2\alpha_k^2\alpha_N^2\cos((\varphi_k - \Phi) - \varphi_N) + \sum_{l=N+1}^{N_r} 2\alpha_N^2\alpha_l^2\cos(\varphi_N - \varphi_l) \tag{4.10}$$

Canceling common terms:

$$\sum_{k=1}^{N-1} \alpha_k^2\cos(\varphi_k - \varphi_N) + \sum_{l=N+1}^{N_r} \alpha_l^2\cos((\varphi_N - \Phi) - \varphi_l)$$

$$\geq$$

$$\sum_{k=1}^{N-1} \alpha_k^2\cos((\varphi_k - \Phi) - \varphi_N) + \sum_{l=N+1}^{N_r} \alpha_l^2\cos(\varphi_N - \varphi_l) \tag{4.11}$$

Change $\varphi'_l - \Phi$ back to φ'_l, for $l < N$

Let $SNR_{N/l}$ be the SNR for changing φ_k into $\varphi_k - \Phi$, except for φ_l, $l < N$. Lemma 4.1 states that $SNR_{N/l} \leq SNR_N$.

$SNR_{N/l} \leq SNR_N$ implies:

$$\sum_{k=1}^{l-1} 2\alpha_k^2\alpha_l^2\cos(\varphi_k - \varphi_l) + \sum_{k=l+1}^{N} 2\alpha_l^2\alpha_k^2\cos(\varphi_l - \varphi_k)$$

$$
\begin{aligned}
&+ \sum_{k=N+1}^{N_r} 2\alpha_l^2\alpha_k^2 \cos\left((\varphi_l - \Phi) - \varphi_k\right) \\
&\geq \\
&\sum_{k=1}^{l-1} 2\alpha_k^2\alpha_l^2 \cos\left((\varphi_k - \Phi) - \varphi_l\right) + \sum_{k=l+1}^{N} 2\alpha_l^2\alpha_k^2 \cos\left(\varphi_l - (\varphi_k - \Phi)\right) \\
&+ \sum_{k=N+1}^{N_r} 2\alpha_l^2\alpha_k^2 \cos\left(\varphi_l - \varphi_k\right)
\end{aligned}
\tag{4.12}
$$

Canceling common terms:

$$
\begin{aligned}
&\sum_{k=1}^{l-1} \alpha_k^2 \cos\left(\varphi_k - \varphi_l\right) + \sum_{k=l+1}^{N} \alpha_k^2 \cos\left(\varphi_l - \varphi_k\right) \\
&+ \sum_{k=N+1}^{N_r} \alpha_k^2 \cos\left((\varphi_l - \Phi) - \varphi_k\right) \\
&\geq \\
&\sum_{k=1}^{l-1} \alpha_k^2 \cos\left((\varphi_k - \Phi) - \varphi_l\right) + \sum_{k=l+1}^{N} \alpha_k^2 \cos\left(\varphi_l - (\varphi_k - \Phi)\right) \\
&+ \sum_{k=N+1}^{N_r} \alpha_k^2 \cos\left(\varphi_l - \varphi_k\right)
\end{aligned}
\tag{4.13}
$$

Given $\varphi_l \geq \varphi_N$, compare Eq.(4.13) with Eq.(4.15). Firstly:

$$
\begin{aligned}
&\sum_{k=1}^{l-1} \alpha_k^2 \cos\left(\varphi_k - \varphi_l\right) + \sum_{k=l+1}^{N} \alpha_k^2 \cos\left(\varphi_l - \varphi_k\right) \\
&- \sum_{k=1}^{N-1} \alpha_k^2 \cos\left(\varphi_k - \varphi_N\right) \\
&\geq \alpha_N^2 \cos\left(\varphi_l - \varphi_N\right) - \alpha_l^2 \cos\left(\varphi_l - \varphi_N\right)
\end{aligned}
\tag{4.14}
$$

Secondly:

$$
\sum_{k=1}^{l-1} \alpha_k^2 \cos\left((\varphi_k - \Phi) - \varphi_l\right) + \sum_{k=l+1}^{N} \alpha_k^2 \cos\left(\varphi_l - (\varphi_k - \Phi)\right)
$$

$$
\begin{aligned}
& - \sum_{k=1}^{N-1} \alpha_k^2 \cos\left((\varphi_k - \Phi) - \varphi_N\right) \\
& \leq \alpha_N^2 \cos\frac{2\pi}{M} - \alpha_I^2 \cos\frac{2\pi}{M}
\end{aligned}
\tag{4.15}
$$

As $\varphi_I - \varphi_N \leq \frac{2\pi}{M}$, Eq.(4.16) $\leq$ Eq.(4.17).

Thirdly:

$$
\begin{aligned}
& \sum_{k=N+1}^{N_r} \alpha_k^2 \cos\left(\varphi_I - \varphi_k\right) \\
& \leq \\
& \sum_{k=N+1}^{N_r} \alpha_k^2 \cos\left(\varphi_N - \varphi_k\right)
\end{aligned}
\tag{4.16}
$$

and

$$
\begin{aligned}
& \sum_{k=N+1}^{N_r} \alpha_k^2 \cos\left((\varphi_I - \Phi) - \varphi_k\right) \\
& \geq \\
& \sum_{k=N+1}^{N_r} \alpha_k^2 \cos\left((\varphi_N - \Phi) - \varphi_k\right)
\end{aligned}
\tag{4.17}
$$

Given Eq.(4.13) to be true and using Eq.(4.16) to Eq.(4.19), Eq.(4.15) is also true, Lemma 4.1 is correct.

In the same manner the following lemma can be proven:
Lemma 4.2: If changing φ'_k into $\varphi'_k + \Phi$, for $k = N_r, N_r - 1, \ldots N$ implies $SNR'_N \geq SNR'_M$, $M > N$. Changing $\varphi_l + \Phi$ back to φ_l, for $l > N$ implies the SNR at the output of the receiver to be less or equal than SNR'_N.

As changing φ_k into $\varphi_k - \Phi$, for $k = 1 \ldots N$, is equivalent with changing φ_l into $\varphi_l + \Phi$, for $l = N_r, N_r - 1, \ldots, N + 1$ and given Lemma 4.1 and Lemma 4.2 to be correct, the optimized rounding algorithm is expected to result in an optimum SNR at the output of the receiver.

The performance of the rounding method and optimized rounding method versus the DOA is given in Figure 4.2. The performance is calculated using an 8 antenna receiver without noise. The average gain achieved using the rounding method is 8.87 dB, for the optimized rounding method 8.88 dB.

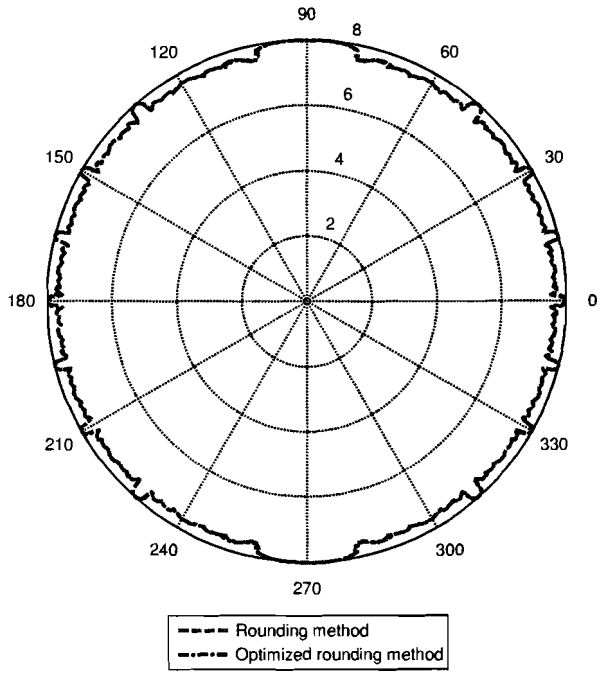

Figure 4.2: Maximization of SNR beamforming performance

4.3 Maximization of SNR beamforming algorithms

The above described methods can be represented in a flowchart. Figure 4.3 shows the flowchart for the Walsh-Hadamard channel estimation. Figure 4.4 the partial Walsh-Hadamard channel estimation and 4.5 and 4.6 show the rounding method beamforming algorithm flowchart and optimized rounding method beamforming algorithm flowchart respectively.

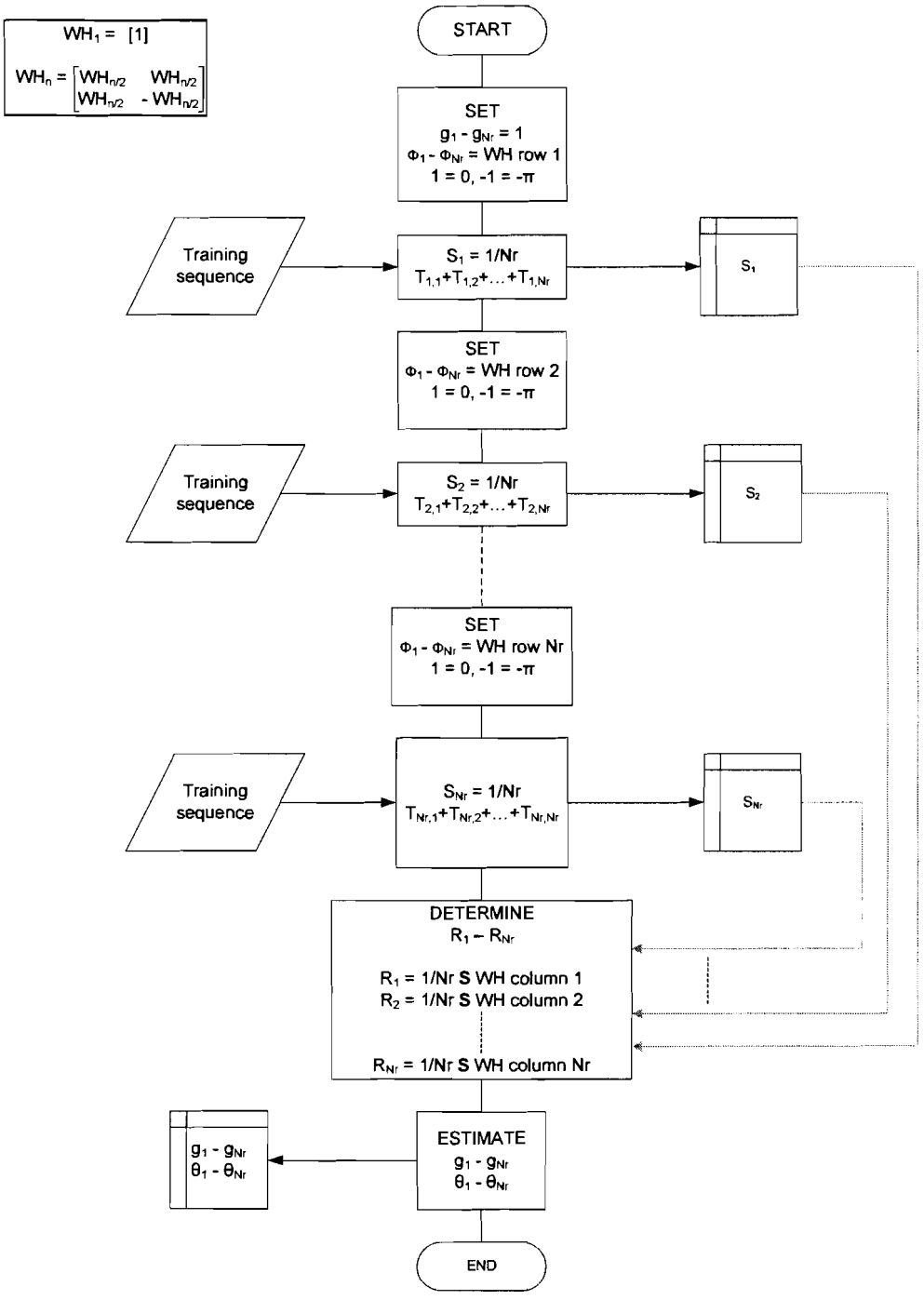

Figure 4.3: Flowchart for Walsh-Hadamard channel estimation

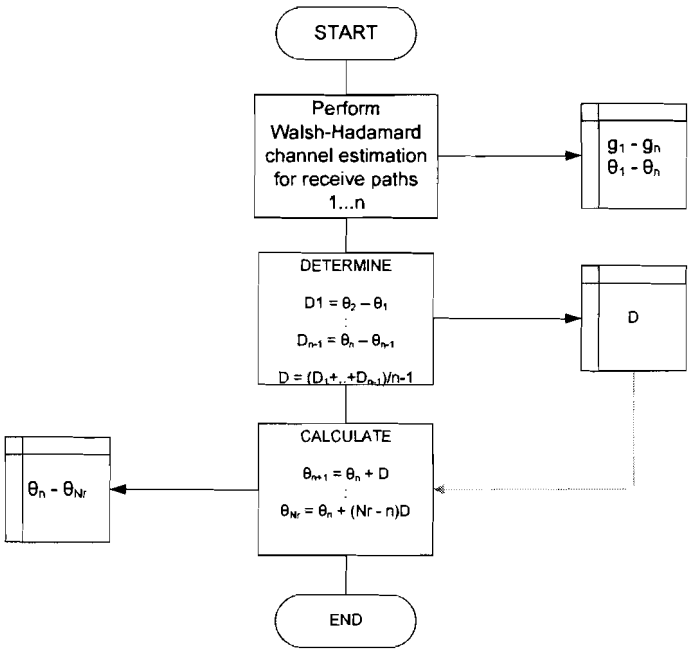

Figure 4.4: Flowchart for partial Walsh-Hadamard channel estimation

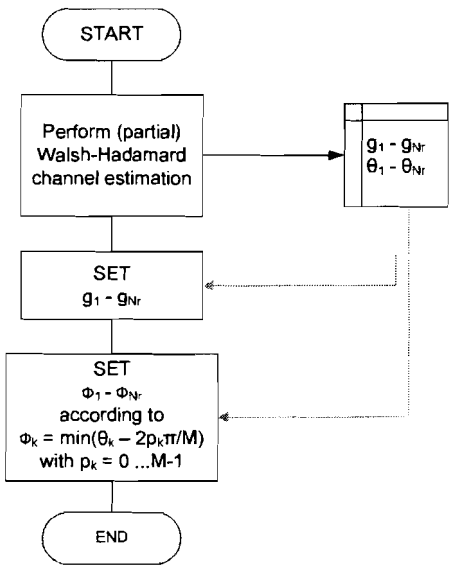

Figure 4.5: Flowchart for rounding method beamforming

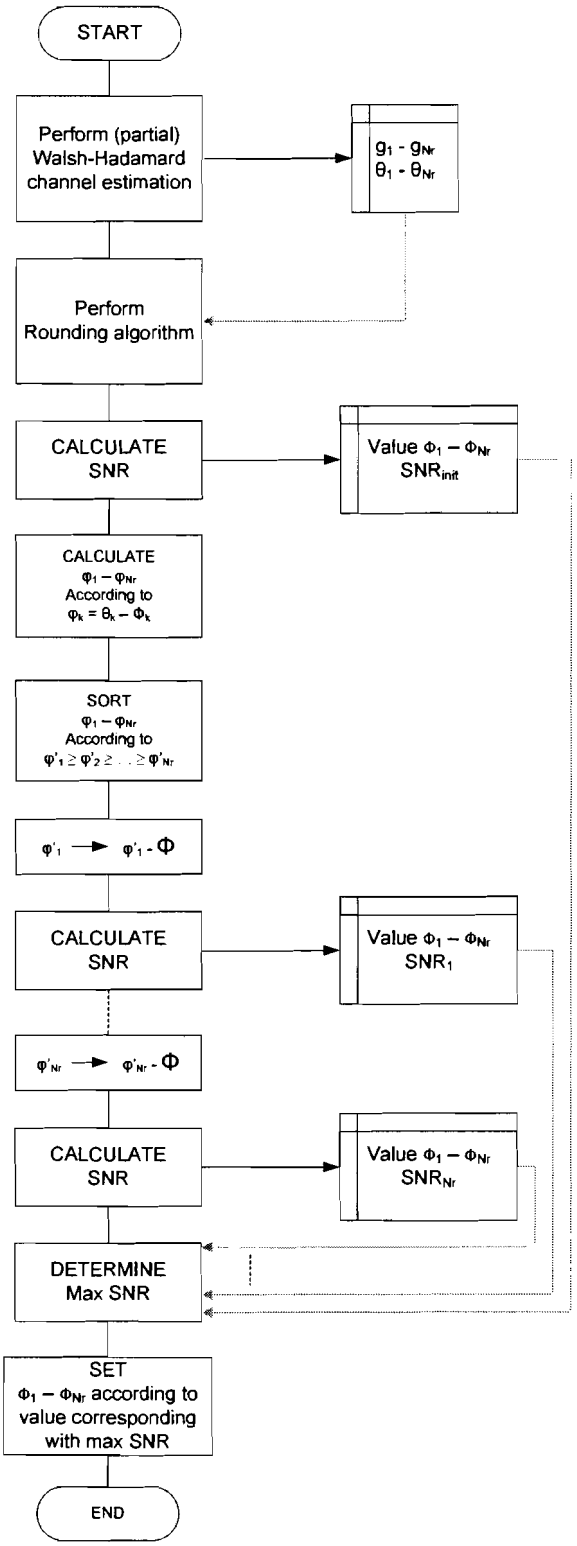

Figure 4.6: Flowchart for optimized rounding method beamforming

Chapter 5

Power controlled beamforming

The beamforming algorithms based upon maximization of SNR beamforming, as developed in Chapter 4, require the channel statistics to be known. To estimate these statistics from the received training symbols, processing time and memory allocation is needed.

In this chapter two beamforming algorithms will be described, which are based upon power controlled beamforming. This form of beamforming does not need the channel statistics to be known but performs beamforming based upon received signal power, as described in Chapter 3.

For this type of beamforming the antenna array specifications, number of antennas (N_r) and distance between the antennas (d), must be known. The effects of changing N_r and d will be discussed in section 5.1, beamforming patterns. Section 5.2 and 5.3 will describe two beamforming algorithm based upon power controlled beamforming.

5.1 Beamforming patterns

The beamforming pattern of an antenna array depends on the number of antennas, N_r, and the antenna spacing, d. As with reference signal beamforming the channel gain is not estimated, all receive path weights will be set to 1. The effect of changing N_r and d is shown in Figure 5.1 for DOA $\beta_0 = 0$, where $L_r = \frac{dN_r}{\lambda} = 2$.[Tse and Viswanath, 2005]

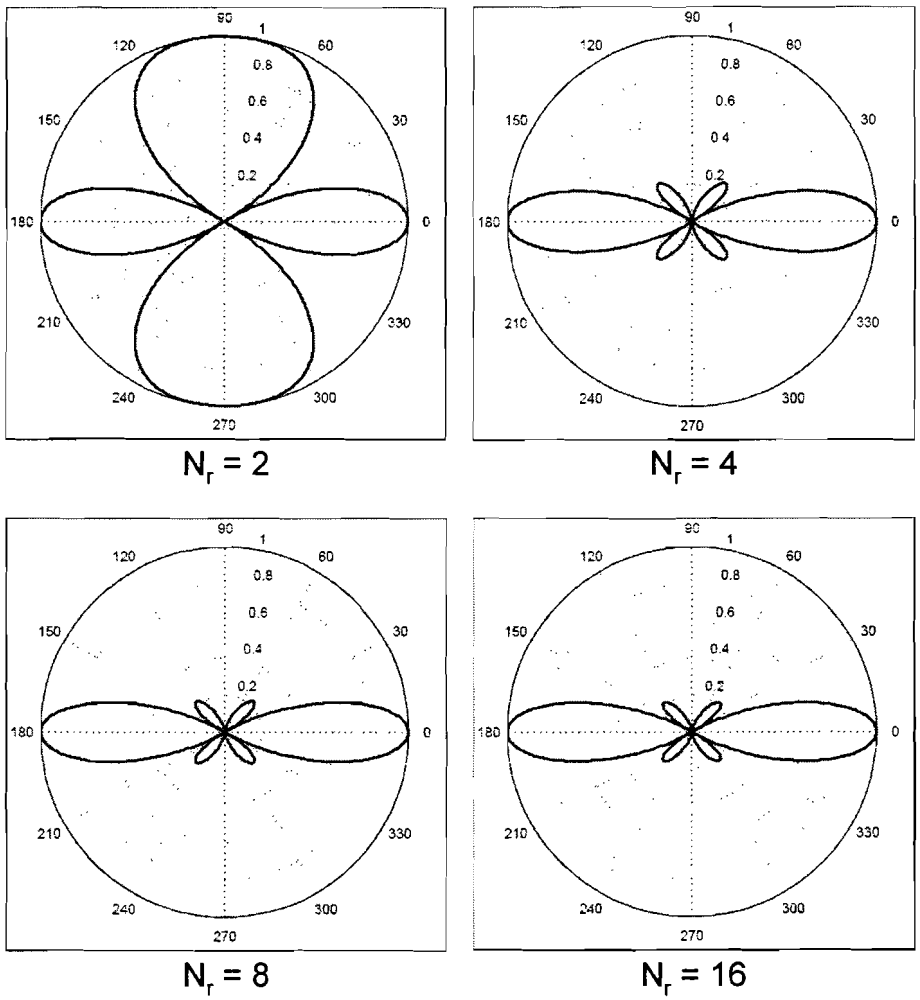

Figure 5.1: Receive beamforming patterns for $L_r = 2$ and $DOA = 0$

From Figure 5.1 the following can be derived:

1. If the beam is directed to a DOA β_0, the beam pattern has main lobes around β_0 and also around any angle β for which

$$\sin\beta \quad = \quad (\sin\beta_0)\ mod\frac{\lambda}{d} \tag{5.1}$$

   If antenna separation d is equal or less than $\frac{\lambda}{2}$, there are only two main lobes. If the antenna separation is greater than $\frac{\lambda}{2}$, then there can be more than one pair of main lobes.

2. The width of the main lobe depends on the length of the antenna array,

L_r. For a fixed L_r, increasing the number of receive antennas does not change the beam width.

To minimize the interference of other signals due to multiple pairs of main lobes and to minimize the size of the antenna array, an antenna separation of $\frac{\lambda}{2}$ is chosen while developing the power controlled beamforming algorithms. The effect of a fixed antenna separation while changing the number of antennas, implying a different L_r, is shown in Figure 5.2 for DOA $\beta = 0$ and $d = \frac{\lambda}{2}$.

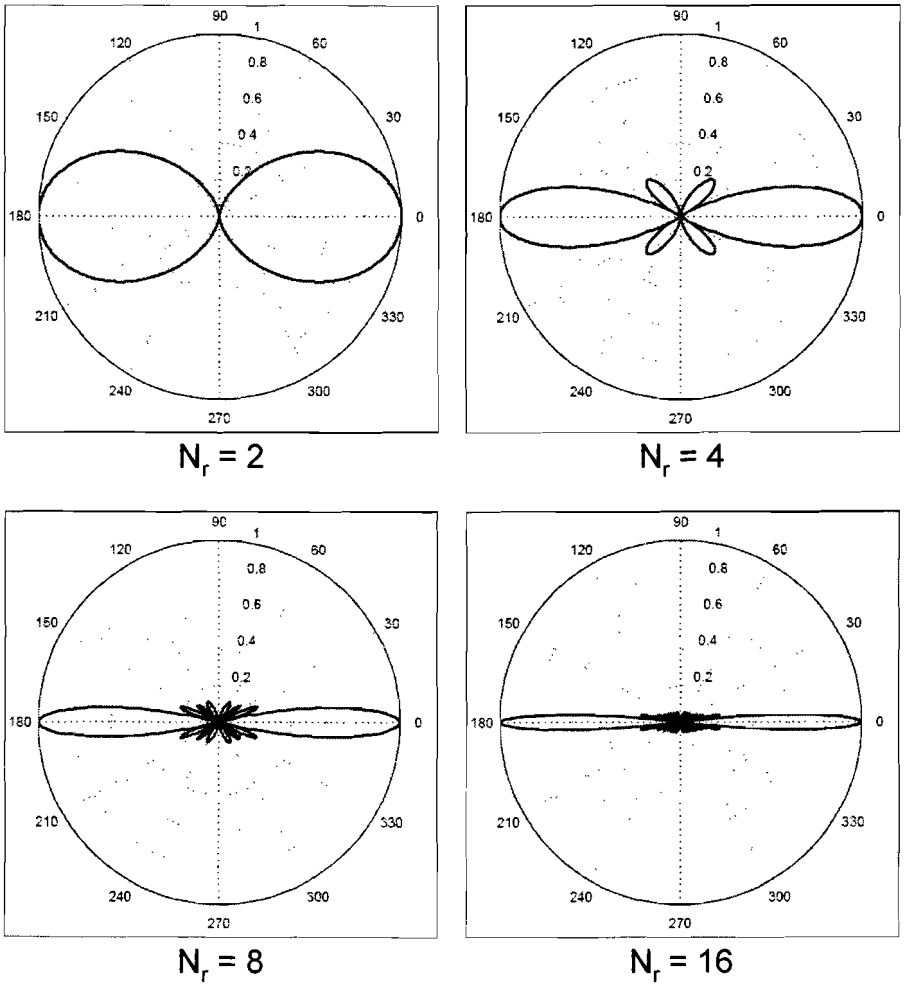

Figure 5.2: Receive beamforming patterns for $d = \frac{\lambda}{2}$ and $DOA = 0$

Both Figure 5.1 and Figure 5.2 show the antenna beam normalized to the maximum antenna gain. The maximum antenna gain is relative to the number of antennas, e.g. if $N_r = 8$ the maximum antenna gain equals 9.03 dB. For a power controlled beamforming algorithm a consideration should be made be-

tween desired achievable antenna gain (hence the number of antennas), beam width and number of training symbols.

5.2 Power controlled beamforming methods

5.2.1 Linear search beamforming

The first power controlled beamforming algorithm is based upon a linear search. From a number of received training symbols the average received power is calculated. Each training symbol is received using a different set of phase shift settings in the receive paths. When all training symbols are received the algorithm selects the best set of phase shift settings, hence the setting in which the maximum average power is received.

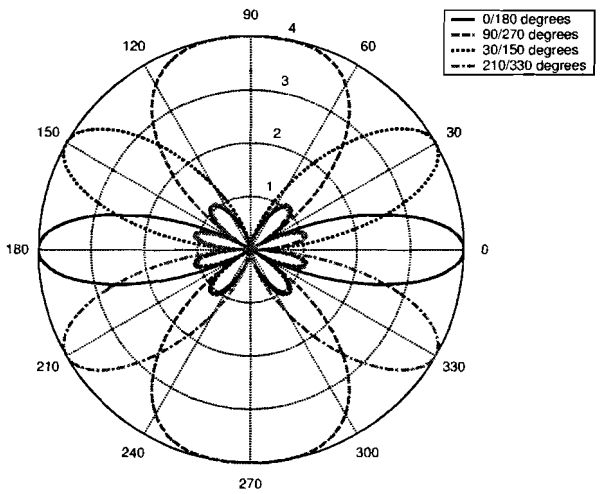

Figure 5.3: Coverage of linear search beamforming for 4 antennas and 4 training symbols

Method

The linear search beamforming algorithm uses a number of training symbols to find the best phase shift setting for the receive paths. The number of training symbols is based upon the knowledge of the antenna array. In T training symbols the set of phase shifts for each receive path, $P(t)$ with index t the t^{th} training symbol, is set such that the beam patterns related to all sets P covers 360 degrees. Figure 5.3 shows the coverage of a 4 element antenna array and 4 settings of P, equivalent with a beam in the direction of: 0 / 180 degrees,

90 / 270 degrees, 30 / 150 degrees and 210 / 330 degrees. After each training symbol the average received power is calculated.

The value of the average power is stored as $m(t)$. After all training symbols are processed, the algorithm determines the maximum of $\mathbf{m}$. The phase shifters in the receive paths are set according to the $P(t)$ related to this maximum.

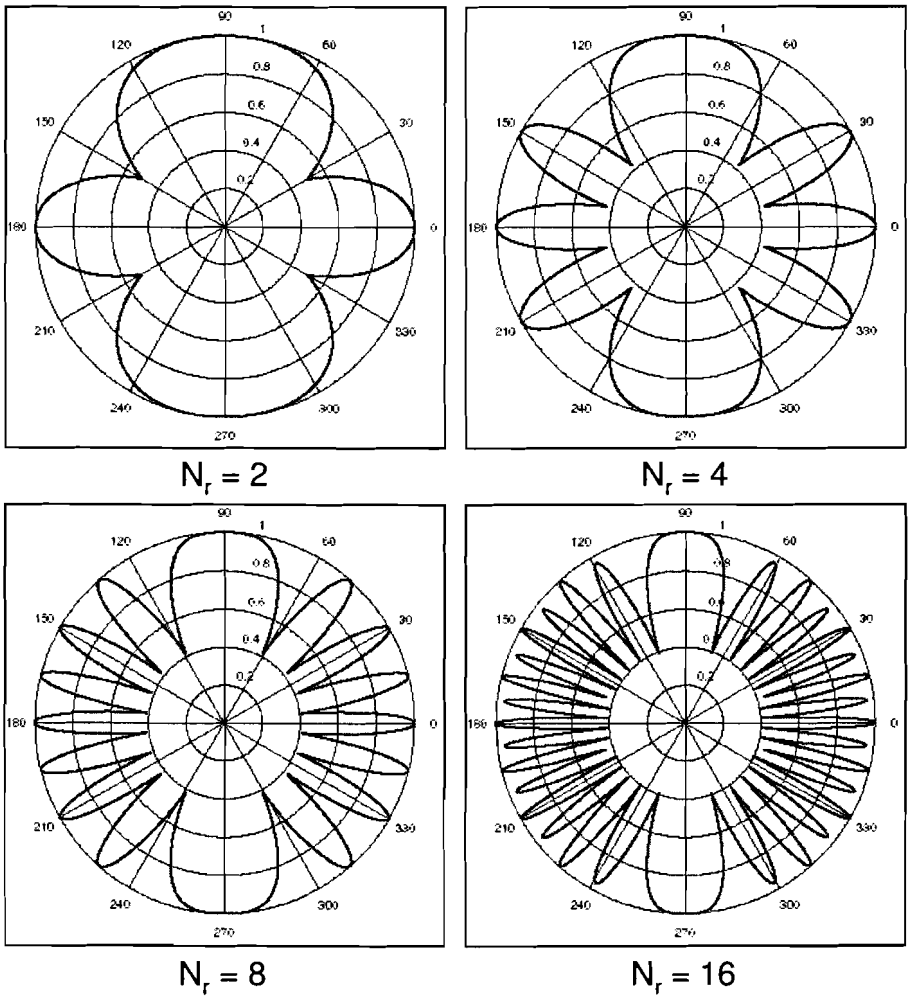

Figure 5.4: Linear search beamforming coverage

Performance

The performance of this method depends on the number of antennas and the number of training symbols. Therefore the performance cannot be expressed in a mathematical manner. If this method is to be compared with the algorithms using channel estimation, the number of training symbols should not exceed the

number of antennas in the antenna array. To evaluate the performance of this algorithm, the linear search beamforming algorithm for a N_r antenna receiver selects the optimum found set P after receiving N_r training symbols.

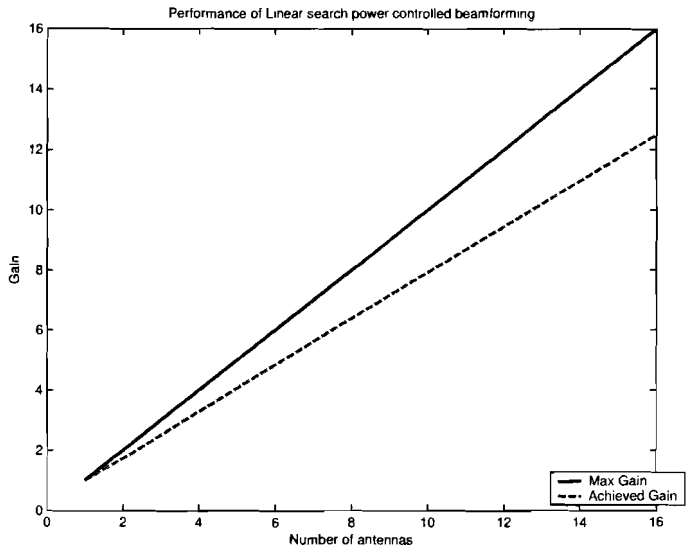

Figure 5.5: Performance of linear search beamforming

Let the DOA vary from 0 to 360 degrees and let no noise be present. Using an antenna array consisting of 2 antennas, and 2 training symbols are sent, the average gain achieved by the algorithm is 2.36 dB, 86% of the maximum achievable gain. Identical for $N_r = 4$ and 4 training symbols, the average achieved gain is 5.16 dB, 82% of the maximum achievable gain. Figure 5.4 and 5.5 show the antenna coverage for DOA from 0 to 360 degrees and algorithm performance for $N_r = 1, 2, 4, 8, 16$, based on average gain versus maximum achievable gain.

5.2.2 Binary search beamforming

Section 5.1 shows that applying more antennas in an antenna array, with a fixed distance d, the beam pattern becomes narrower. Using the linear search beamforming algorithm, more training symbols need to be sent in order find a satisfying solution. The second power controlled beamforming algorithm can be best described as a binary search method. The algorithm performs a number of iteration, each time narrowing the possibilities of the direction from which the signal is received. Each iteration uses more antennas of the antenna array than the preceding step, hence narrowing the beam.

Method

Each iteration in this method uses more antennas of the antenna array than the preceding step. The first iteration of this method uses the linear reference signal beamforming algorithm for an antenna array with 4 antennas and 4 training symbols. The next iteration increases the number of used antennas, however only performs the reference signal beamforming algorithm in the direction of the best result found in the previous iteration. Figure 5.6 shows the result of the second iteration when using 8 antennas and 3 training symbols, after the first iteration resulted in a DOA of 0 / 180 degrees. If the number of iterations grows, the DOA can be approximated more accurately.

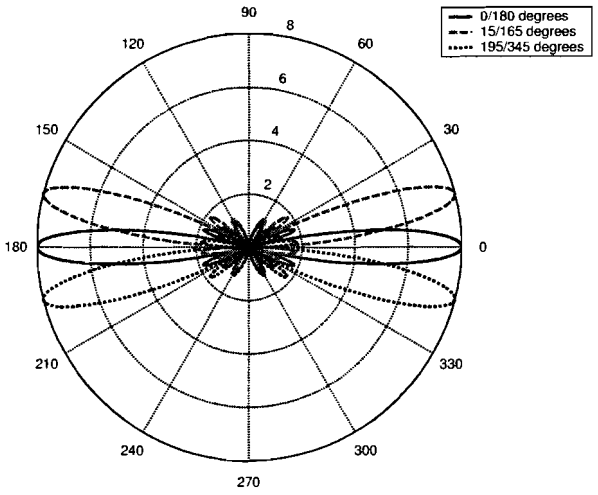

Figure 5.6: 2nd iteration for 8 antenna binary search beamforming

Performance

Under the same restriction that the number of training symbols is equal or less than the number of antennas, this algorithm does not improve the performance if 4 antennas or less are used in the array. In the case of 8 antennas, after the first iteration, the second iteration uses 8 antennas and again 4 training symbols. This method achieves 90% of the maximum gain. Compared to the 80% with the linear reference signal beamforming algorithm an improvement of 11%. If the antenna array consists of 16 antennas, this method can execute the first and second iteration as for the 8 antenna array. The third iteration can exploit 16 antennas and using 4 training symbols, an average gain of 11.79 dB is achieved, 94% of the maximum gain only using 12 training symbols. Compared to the 78% in the linear reference signal beamforming case an improvement of 20%.

Figures 5.7 and 5.8 show the result of the binary reference signal beamforming algorithm compared to the linear reference signal beamforming algorithm for 8 and 16 antennas versus the DOA, in a no noise environment.

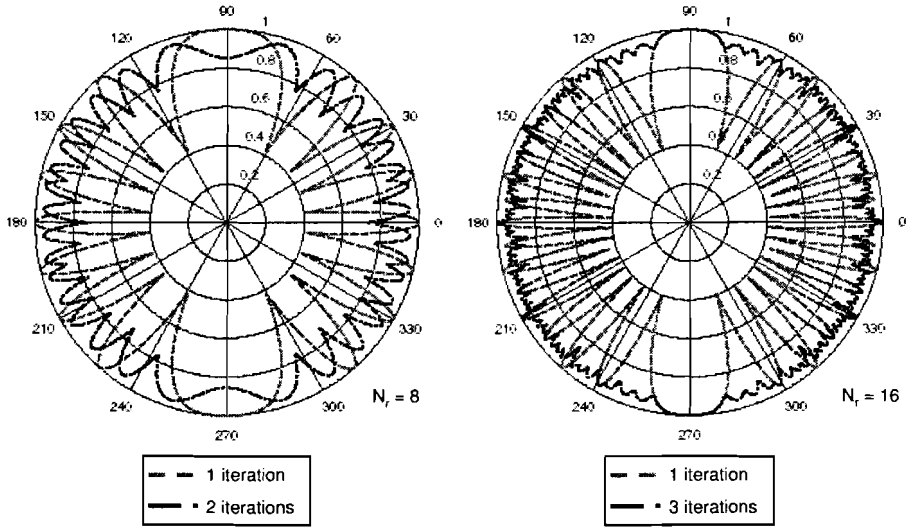

Figure 5.7: Normalized gain for linear and binary search beamforming vs. DOA

5.3 Power controlled beamforming algorithms

Figure 5.9 shows the flowchart for the linear search beamforming algorithm, Figure 5.10 shows the flowchart for the binary search beamforming algorithm.

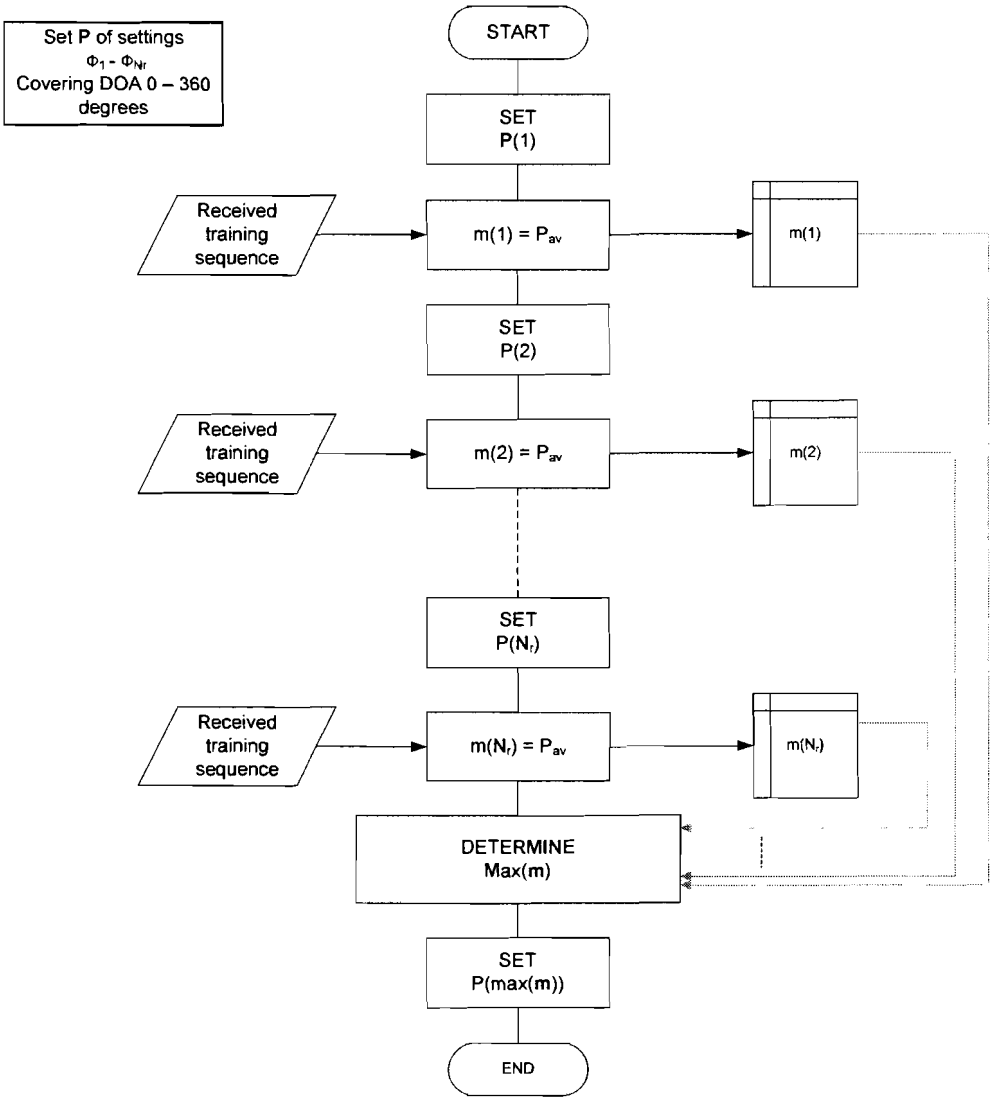

Figure 5.8: Linear search beamforming algorithm

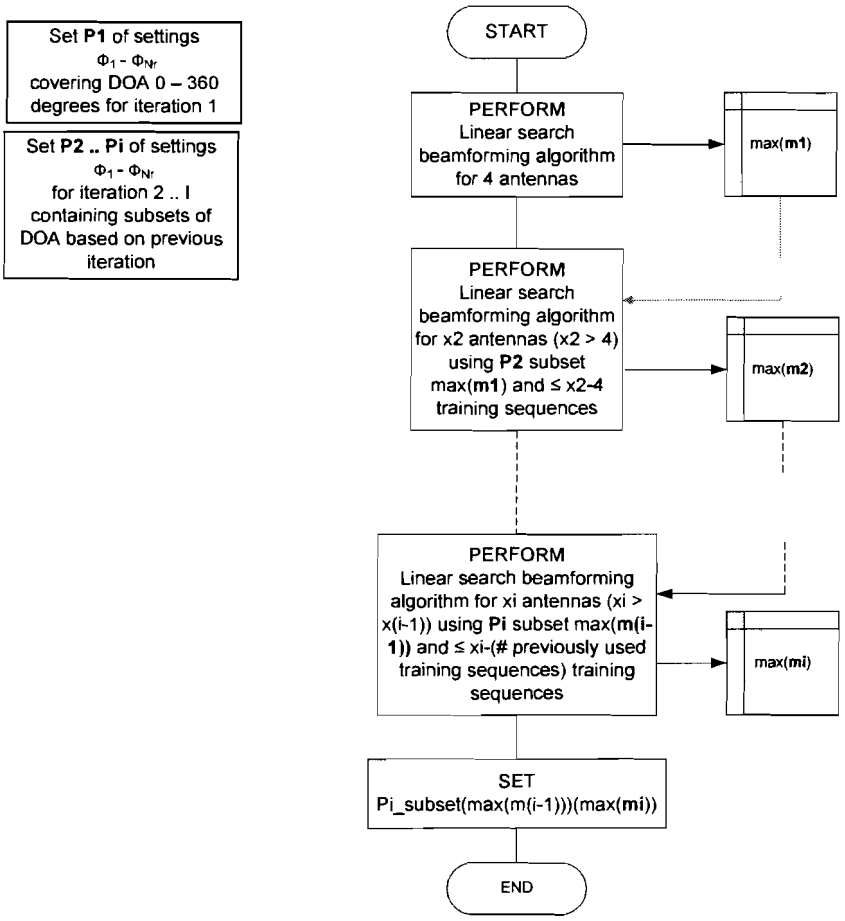

Figure 5.9: Binary search beamforming algorithm

Chapter 6

Simulation results

Chapter 4 and 5 describe 4 beamforming algorithms and their performance under ideal circumstances, no noise and no analog-to-digital conversion. In this chapter the algorithm performance is given, firstly showing the effects of analog-to-digital conversion on the algorithms in a no noise situation. As analog-to-digital conversion is part of the receiver design and an ADC should be dimensioned based on the output signal of the RF front-end, further simulations are performed without analog-to-digital conversion. Secondly the beamforming algorithms are simulated introducing AWGN. Following sections describe the simulation environment, ADC simulation and simulation of the maximization of SNR beamforming algorithms and reference signal beamforming algorithms.

6.0.1 Simulation environment

All simulations are performed at equivalent baseband level. Using the following values:

1. The DOA is chosen randomly, uniformly distributed between 0 and 2π.
2. Simulations are performed using the complex envelope of the received signal
3. The training symbol is a BPSK (binary phase shift keying) signal. The training symbol is sampled 500 times.
4. The received training symbol at antenna k, RT_k, with $k = 1 \ldots N_r$, is the training symbol with a phase shift θ_k based on the DOA
5. Phase shift ϕ in the receive path can be set in multiples of $\pi/4$, hence $\phi_k = M\pi/4$, with $M = 0, \ldots 7$, unless stated otherwise
6. Performance figures are based on 250,000 simulations

6.0.2 Analog-to-digital conversion

If the analog output of the RF front-end, an in-phase and quadrature baseband signal, is converted into a digital signal, quantization noise is introduced. The level of quantization noise depends on the number of bits used to describe the signal. Figure 6.1 and 6.2 show the performance of maximization of SNR beamforming and power controlled beamforming if an ADC is used with 16, 32, 64 and 128 quantization levels (4, 5, 6 and 7 bits respectively). The receiver consists of an 8 element antenna array.

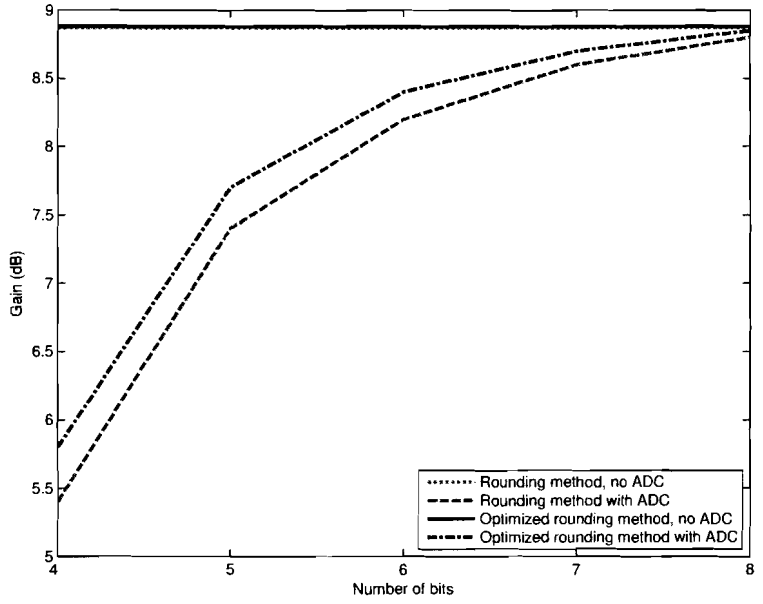

Figure 6.1: Effect of ADC on maximization of SNR beamforming performance

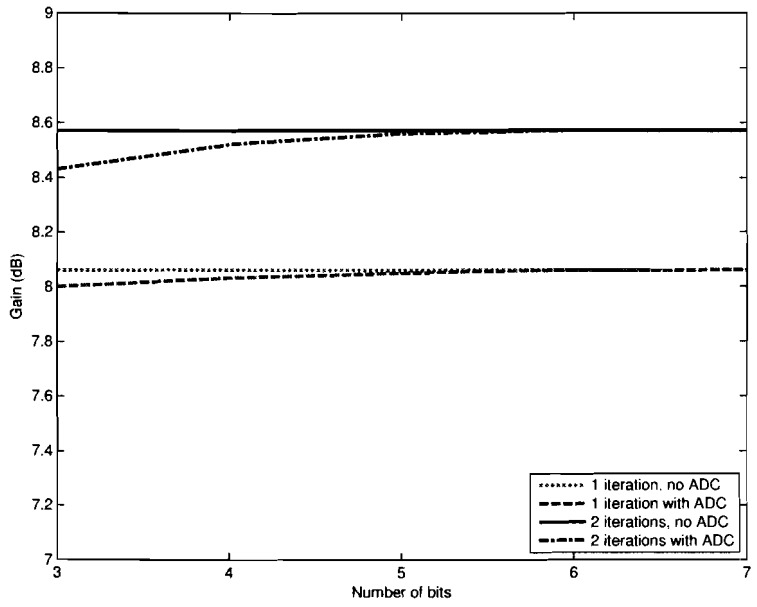

Figure 6.2: Effects of ADC on power controlled beamforming performance

6.0.3 Noise performance

This section shows the performance of maximization of SNR beamforming and power controlled beamforming for a received signal with complex noise. Noise n is generated using two statistically independent random variables (n_1 and n_2), each normally distributed with mean 0 and variance 1, $n = n_1 + in_2$. The complex noise array has the same length as the training symbol and is dimensioned such that the average noise power P_{noise} and P_{sig} are related as follows:

$$SNR = 10log_{10}(\frac{P_{sig}}{B\,P_{noise}})$$

The received training symbol with noise at antenna k, RTN_k, with $k = 1 \ldots N_r$, is defined as $RTN_k = RT_k + n$. Figures 6.3 and 6.4 show the noise performance of maximization of SNR beamforming with $N_r = 8$ and $N_r = 16$ respectively. Figure 6.5 shows the noise performance for an 8 antenna receiver and maximization of SNR beamforming based on partial channel estimation. Finally Figures 6.6 and 6.7 show the noise performance for power controlled beamforming with $N_r = 8$ and $N_r = 16$.

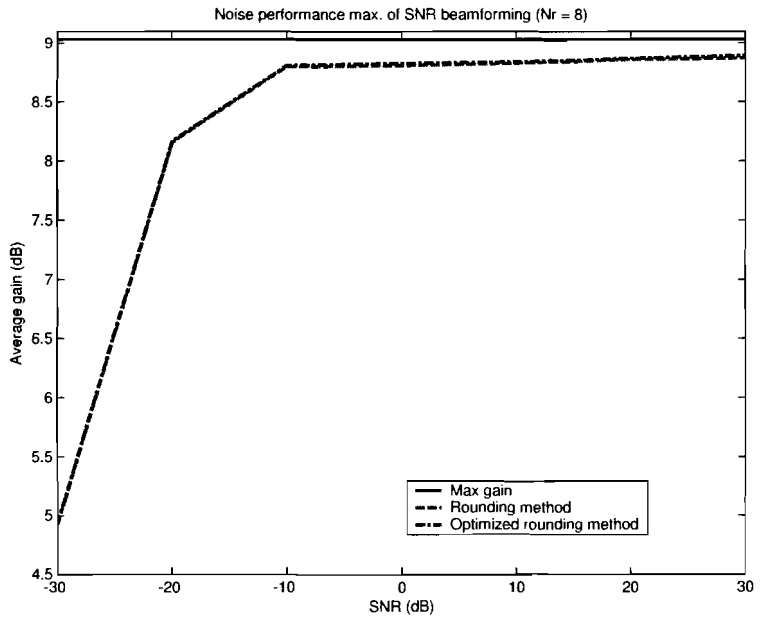

Figure 6.3: Noise performance of maximization of SNR beamforming with $N_r = 8$

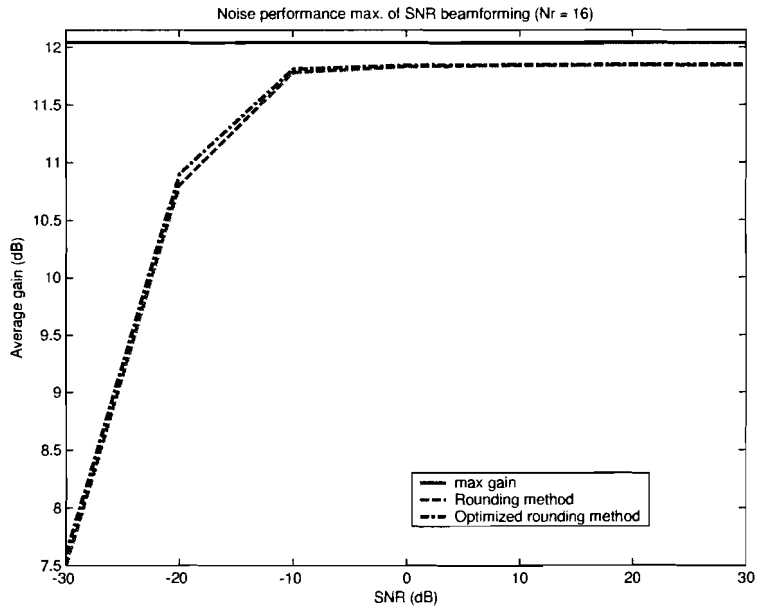

Figure 6.4: Noise performance of maximization of SNR beamforming with $N_r = 16$

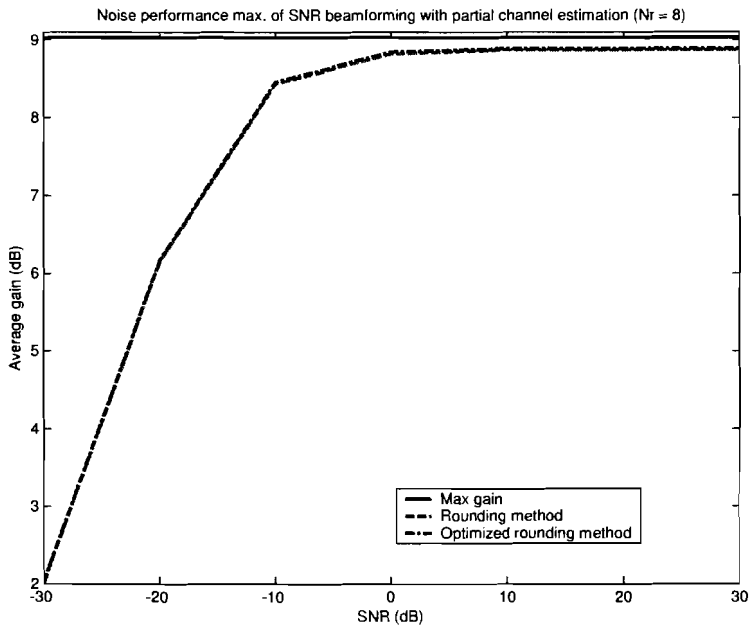

Figure 6.5: Noise performance of maximization of SNR beamforming with partial channel estimation, $N_r = 8$

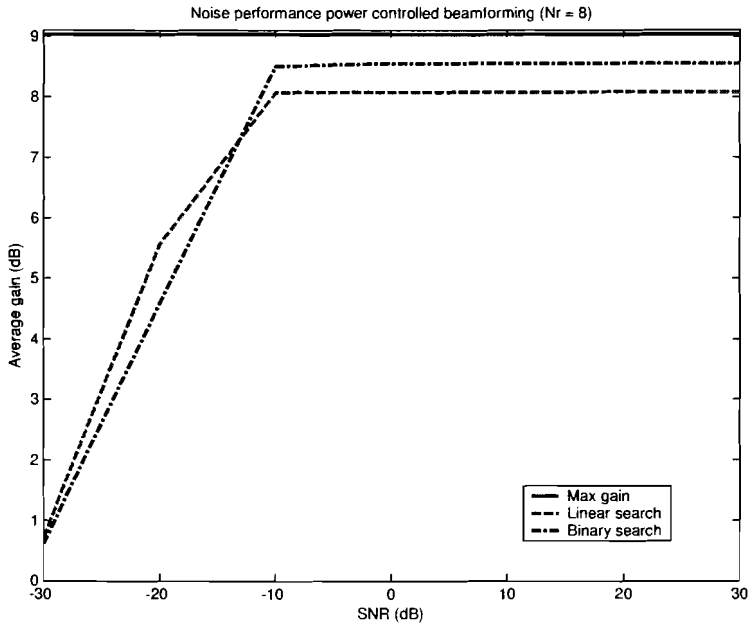

Figure 6.6: Noise performance of power controlled beamforming with $N_r = 8$

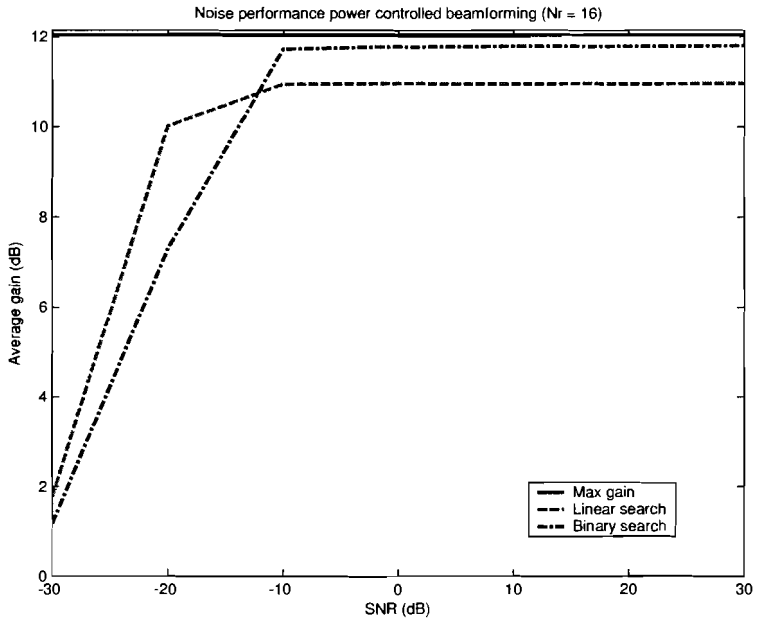

Figure 6.7: Noise performance of power controlled beamforming with $N_r = 16$

6.0.4 Effect of phase shift with steps of $pi/2$

The above performed simulations all used a phase shift step size for ϕ of $\pi/4$. This section shows the effect of increasing the step size to $\pi/2$. The performance is evaluated for an 8 antenna receiver, both for maximization of SNR beamforming as for power controlled beamforming. The results are shown in Figure 6.8 and 6.9 respectively.

6.0.5 Random phase shift

Finally, the performance of the beamforming algorithms is evaluated using a channel with random channel delay, resulting in a phase shift for the complex envelope notation of $e^{j\rho_k}$, with $k = 1 \ldots N_r$ and ρ_k a statistically independent random variable, uniformly distributed between 0 and 2π.

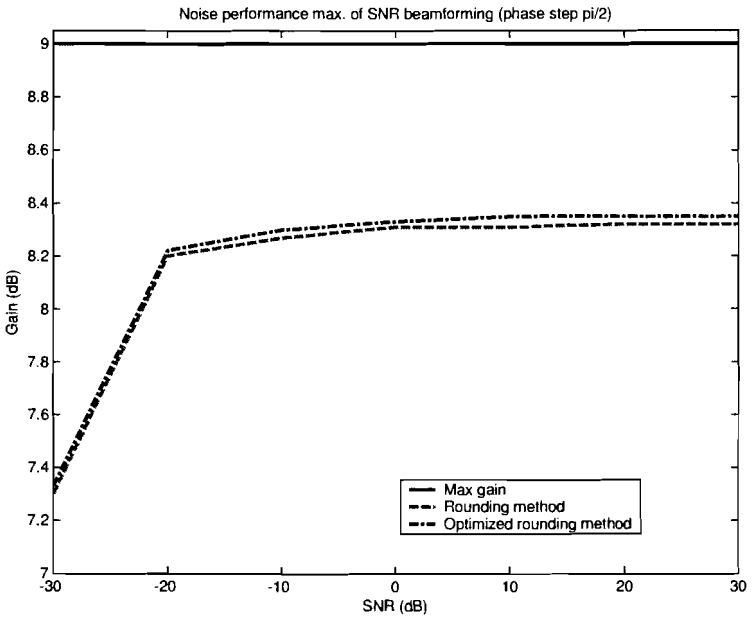

Figure 6.8: Noise performance of maximization of SNR beamforming with $\Phi = \pi/2$

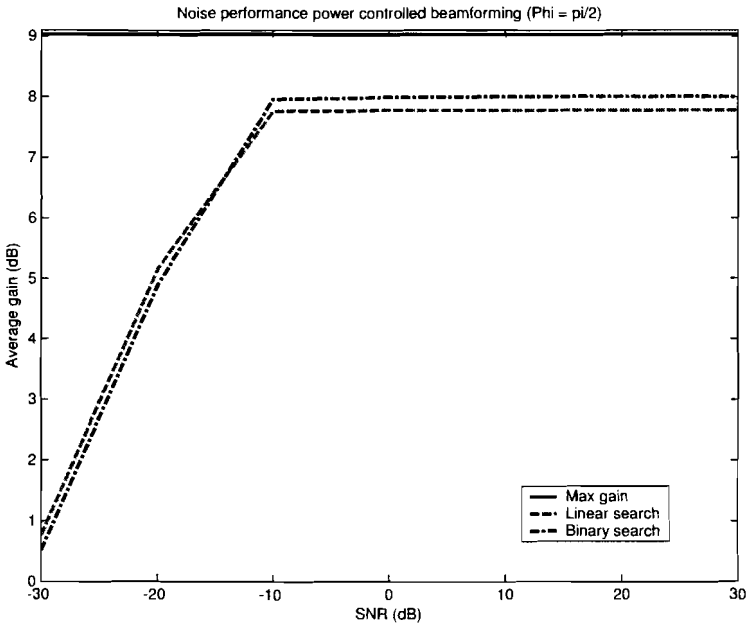

Figure 6.9: Noise performance of power controlled beamforming with $\Phi = \pi/2$

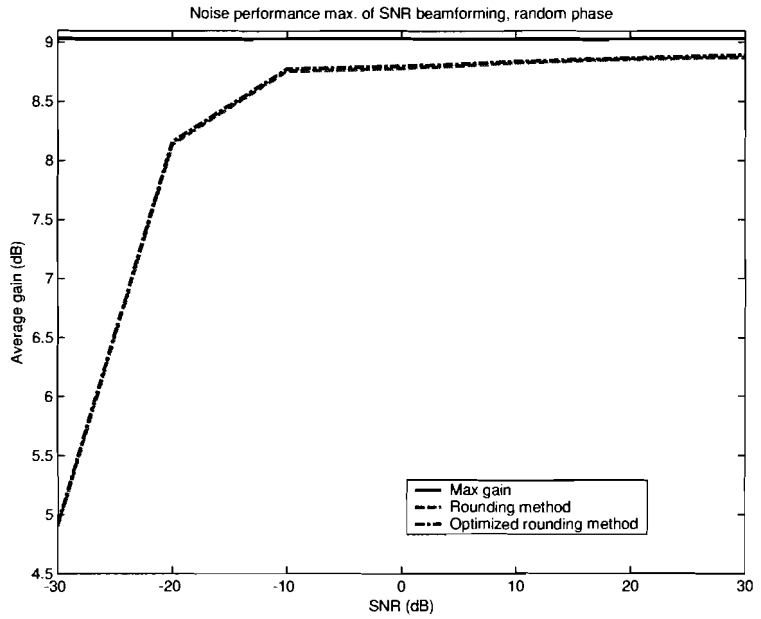

Figure 6.10: Noise performance of max. of SNR beamforming with random signal phase

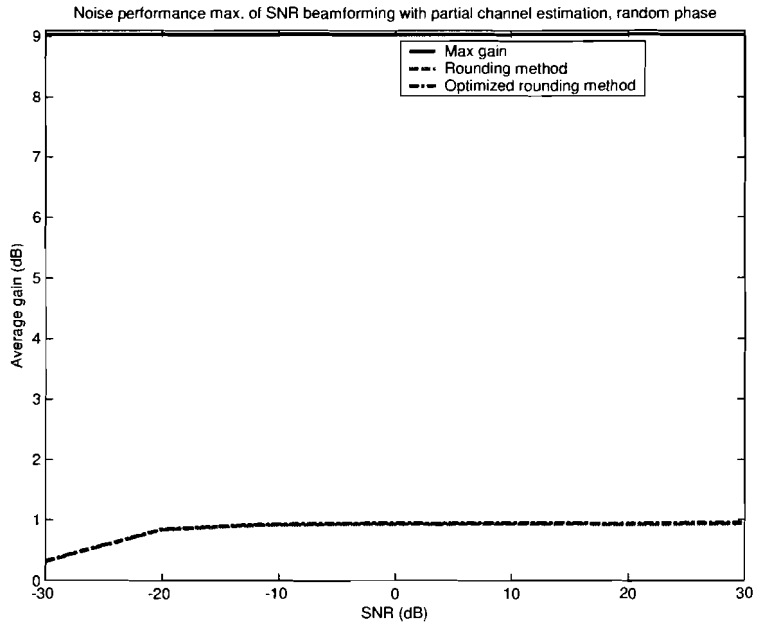

Figure 6.11: Noise performance of max. of SNR beamforming with partial channel estimation and random signal phase

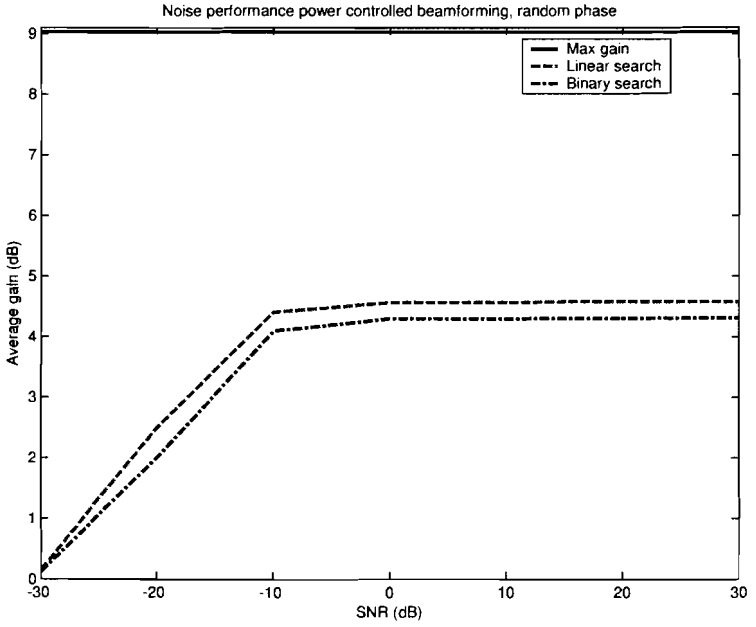

Figure 6.12: Noise performance of power controlled beamforming with random signal phase

Chapter 7

Conclusions and recommendations

This master thesis project has been focussed on the development of adaptive beamforming algorithms. Beamforming is a part of the 60 GHz receiver and is closely related to the other elements of the receiver architecture. At the end of this report some conclusions will be drawn on the beamforming process and recommendations will be made on future developments and integration in the 60 GHz receiver.

7.1 Conclusions

7.1.1 Channel estimation

- Channel estimation using a unitary matrix is capable of estimating gain and phase for each receive path, given the combined digital baseband signal. For this estimation a number of training symbols is needed, equal to the number of antennas.
- Partial channel estimation is only capable of estimating the phase for each receive path. However, if the delay of the received signal is not based on the DOA, this method cannot be used.
- Accuracy of the estimation depends on the number of quantization levels in the AD converter and the number of samples of the training symbol.
- Channel estimation requires processing time and memory allocation.

7.1.2 Maximization of SNR beamforming

- Maximization of SNR beamforming needs accurate channel estimation.
- Rounding method provides accurate beamforming, however, not an optimum combining result.
- Optimized rounding method provides optimum combining result.
- Difference in performance is small.
- Beamforming is also possible if channel statistics differ between the receive paths.
- Beamforming algorithm requires processing time and memory allocation.

7.1.3 Power controlled beamforming

- No channel statistics need to be known, resulting in a smaller processing time- and memory allocation requirement.
- Number of training symbols depends on beam width.
- Binary search algorithm boosts performance over linear search algorithm because of its iterative nature.
- Algorithms cannot be used if channel statistics differ between the receive paths, hence the delay of the received signal is not based on the DOA.

7.2 Recommendations

For possible future research on 60 GHz receivers in general and beamforming algorithms in particular the following recommendations will be given:

- The beamforming algorithms have been developed using a generic receiver architecture. The algorithms need to be adapted when the receiver architecture becomes more concrete.
- Beamforming needs to be implemented in the future standard for wireless communication at 60 GHz.
- Beamforming can be performed at the transmitter side as well. Research is needed how the receiver can provide feedback to the transmitter.
- Beamforming performance can be simulated using a more realistic simulation environment.
- Beamforming in this project was focussed on maximizing the SNR of the received signal. Beamforming can also be used for suppressing interference signals. Research can be done on optimizing SNR and at the same time minimizing interference.

Appendix A

List of abbreviations

ADC Analog-to-Digital Conversion

AWGN Additive White Gaussian Noise

BPSK Binary Phase Shift Keying

DOA Direction Of Arrival

DSP Digital Signal Processing

EGC Equal-Gain Combining

IF Intermediate Frequency

ISI Inter symbol interference

LNA Low-Noise Amplifier

LO Local Oscillator

MAC Medium Access Control

MRC Maximal-Ratio Combining

QAM Quadrature Amplitude Modulation

QoS Quality of Service

RF Radio Frequency

SNR Signal-to-Noise Ratio

UWB Ultra-Wide Band

WLAN Wireless Local Area Network

Appendix B

Bibliography

[1] Koh, Chris
THE BENEFITS OF 60 GHZ UNLICENSED WIRELESS COMMUNICATIONS
Terabeam company paper, no year.

[2] Smulders, P.F.M.
EXPLOITING THE 60 GHZ BAND FOR LOCAL WIRELESS MULTIMEDIA ACCESS: PROSPECTS AND FUTURE DIRECTIONS
IEEE Communications magazine, Jan 2002, Volume 40, Issue 1, P140 - 147.

[3] Haykin, Simon and Moher, Michael
MODERN WIRELESS COMMUNICATIONS Upper Saddle River, New Jersey: Pearson Education, Inc., 2005. (ISBN 0-13-124697-6)

[4] Hajimiri, A., Komijani,A., Natarajan, A., Chunara, R., Guan, X. and Hashemi,H.
PHASED ARRAY SYSTEMS IN SILICON
IEEE Communicatioins magazine, Aug 2004, P122 -130.

[5] van Veen, Barry and Buckley, Kevin M.
BEAMFORMING: A VERSATILE APPROACH TO SPATIAL FILTERING
IEEE ASSP Magazine, Apr 1988, P4 - 24.

[6] Proakis, John G.
DIGITAL COMMUNICATIONS, 4th ed.
New York: McGraw Hill, 2001. (ISBN 0-07-232111-3)

[7] Couch, Leon W.
DIGITAL AND ANALOG COMMUNICATION SYSTEMS, 6th ed.
Upper Saddle River, New Jersey: Pearson Education, Inc., 2001. (ISBN 0-13-081223-4)

[8] Tse, David and Viswanath, Pramod
FUNDAMENTALS OF WIRELESS COMMUNICATIONS
New York: Cambridge University Press, 2005. (ISBN 13-978-0-521-84527-4)

[9] Tanenbaum, Andrew S.
COMPUTER NETWORKS
Upper Saddle River, New Jersey: Pearson Education, Inc., 2003. (ISBN 0 13)